

Doppler perturbations of satellite observations by VHF ST radar

Jordan Jonker¹, Manuel Cervera^{1,2}, Trevor Harris¹, David Holdsworth^{1,2},
Andrew MacKinnon¹, David Neudegg^{1,2}, Iain Reid^{1,3}

¹Department of Physics, The University of Adelaide, Adelaide, SA 5000, Australia

²Defence Science and Technology Group, Edinburgh, SA 5111, Australia

³ATRAD Pty Ltd, Thebarton, SA 5031, Australia



Why use VHF radar for satellite observations?

The number of satellites in Low Earth Orbit (LEO) is exponentially increasing.

Proposed corporate mega constellations mean that there may be an additional 100,000 satellites in LEO, compared to 4871 in 2021.

Increased the risk of Kessler Syndrome events.

VHF radar provides a low-cost alternative to traditional satellite detection methods.



Buckland Park Stratosphere Troposphere (BPST)

VHF radar.

Located ~35 km north of Adelaide.

Operates at 55 MHz at 40 kW.

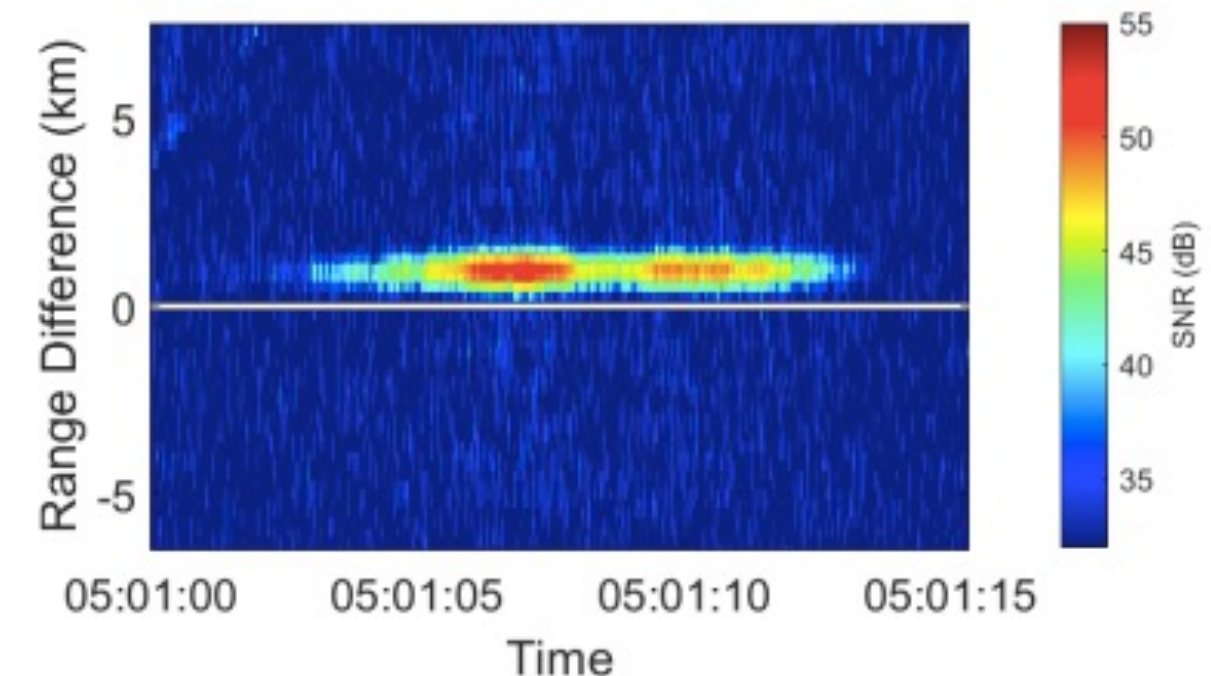
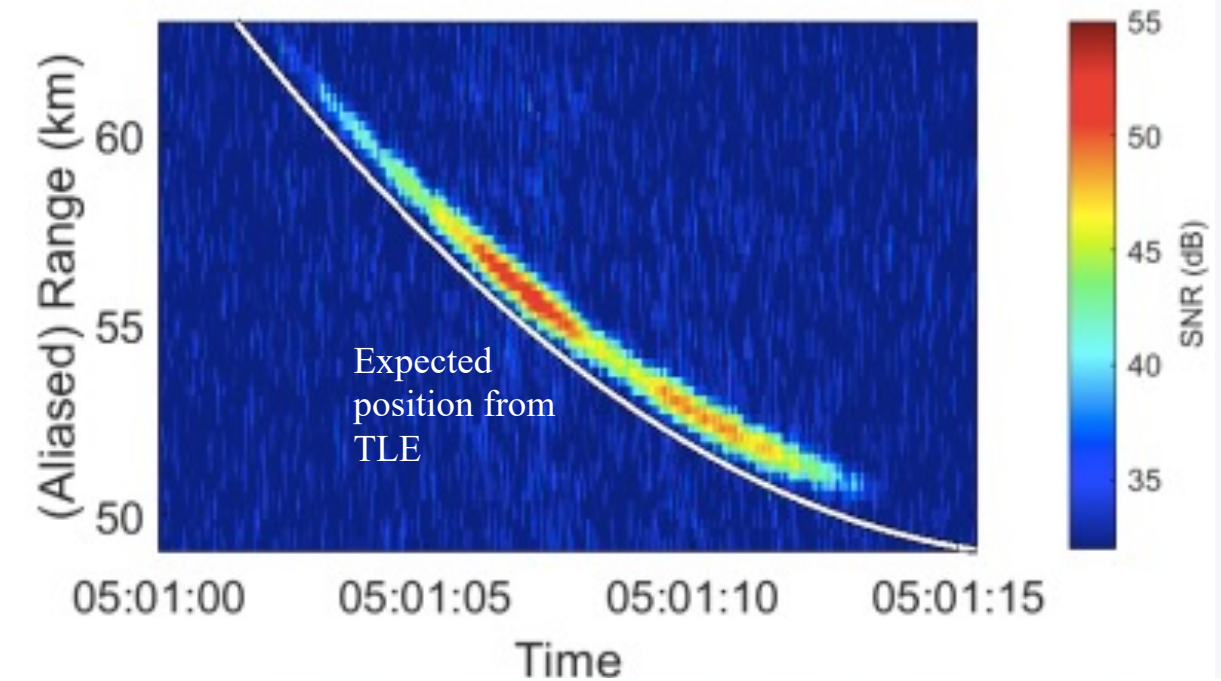
12x12 array of Yagi antennas

-5 beam directions with 6° beam width:

- Vertical

- NESW (15° off Zenith)

Can detect objects with a radar cross section of $1m^2$ at a range of 1000



Courtesy of: Heading et. Al (2022) 

Buckland Park Stratosphere Troposphere (BPST)

VHF radar

Located ~35

Operates at 4

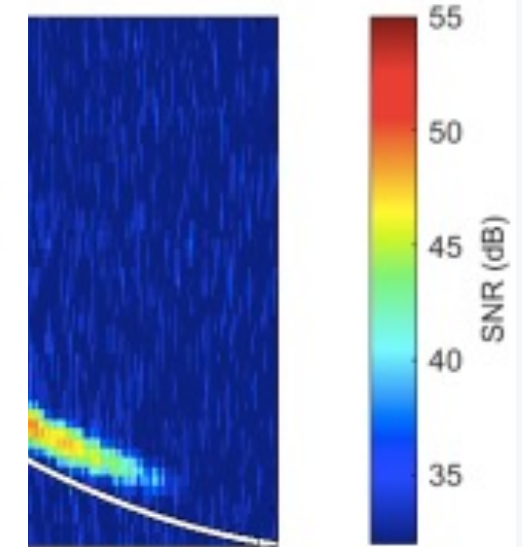
12x12 array

-5 beam

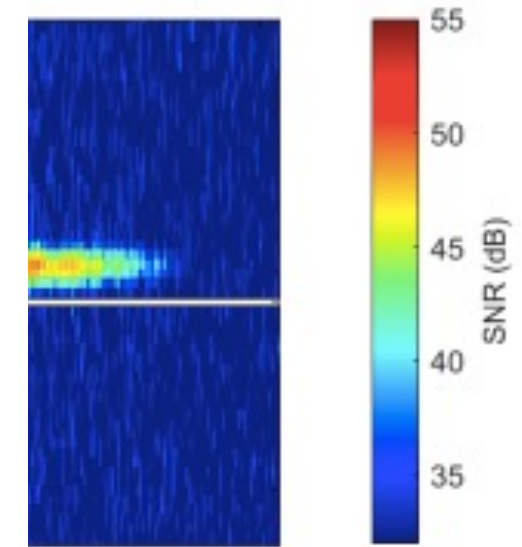
- V

- M

Can detect o



10 05:01:15



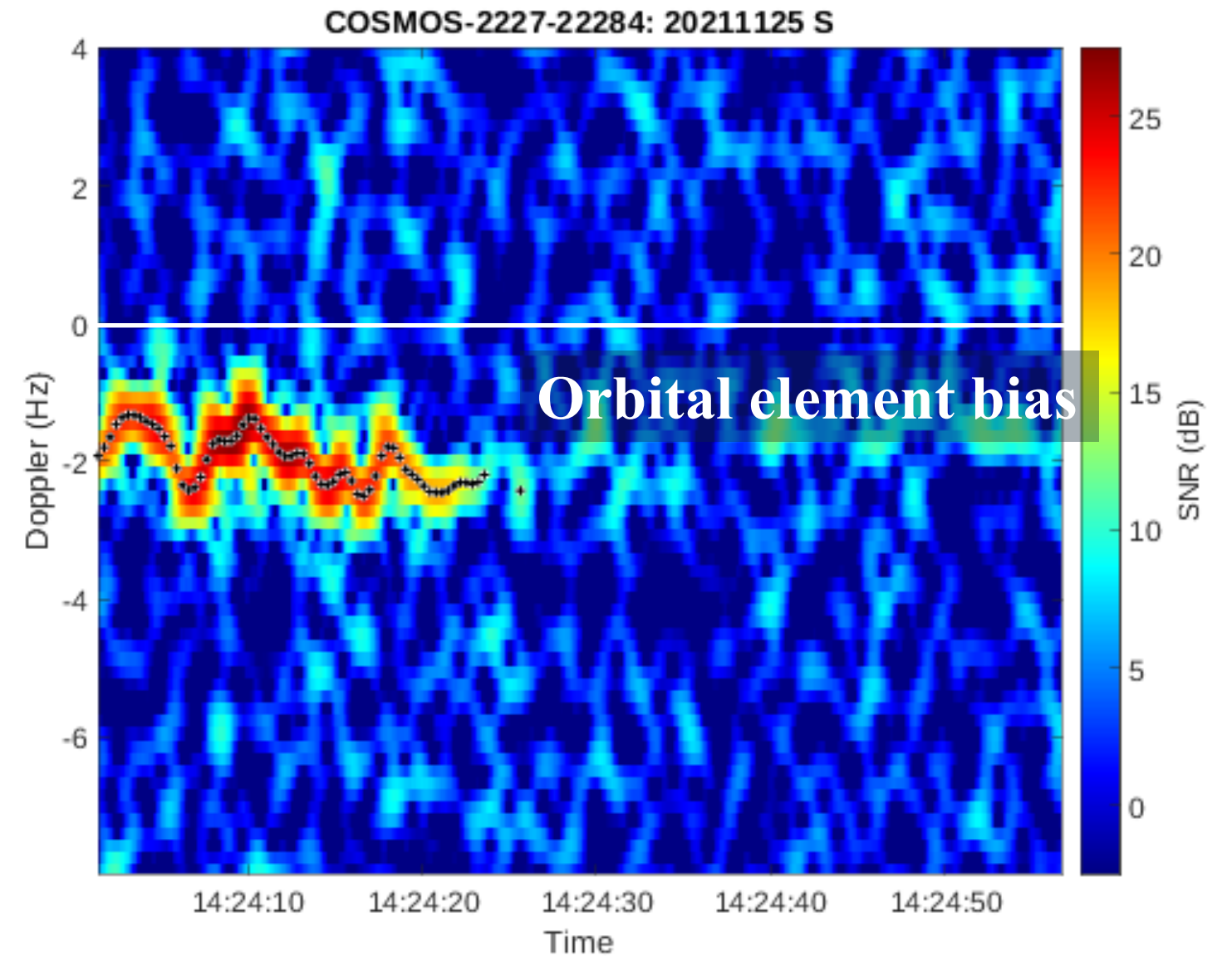
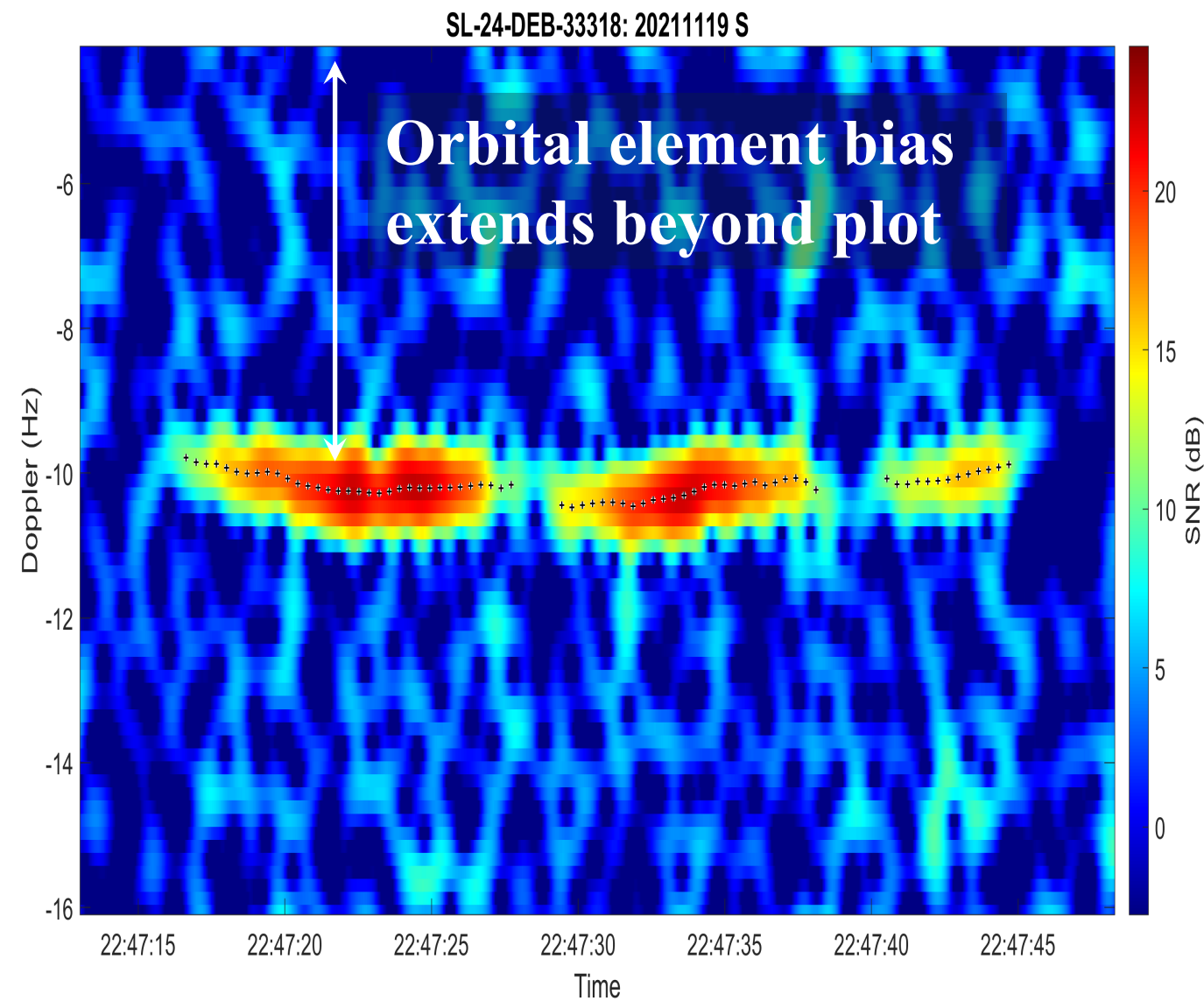
10 05:01:15

Time

Courtesy of: Heading et. Al (2022)

THE UNIVERSITY
of ADELAIDE

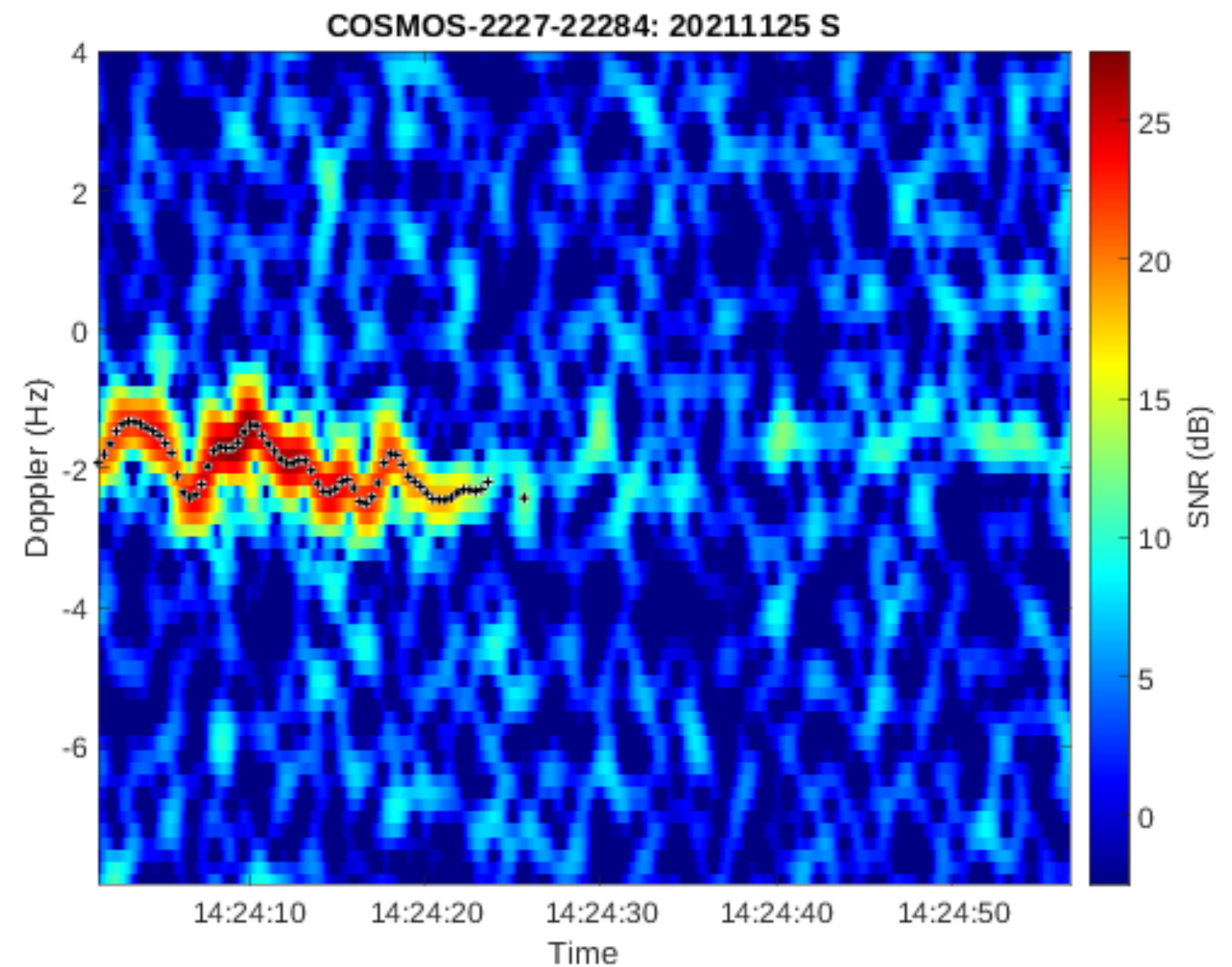
Doppler measurements from BPST

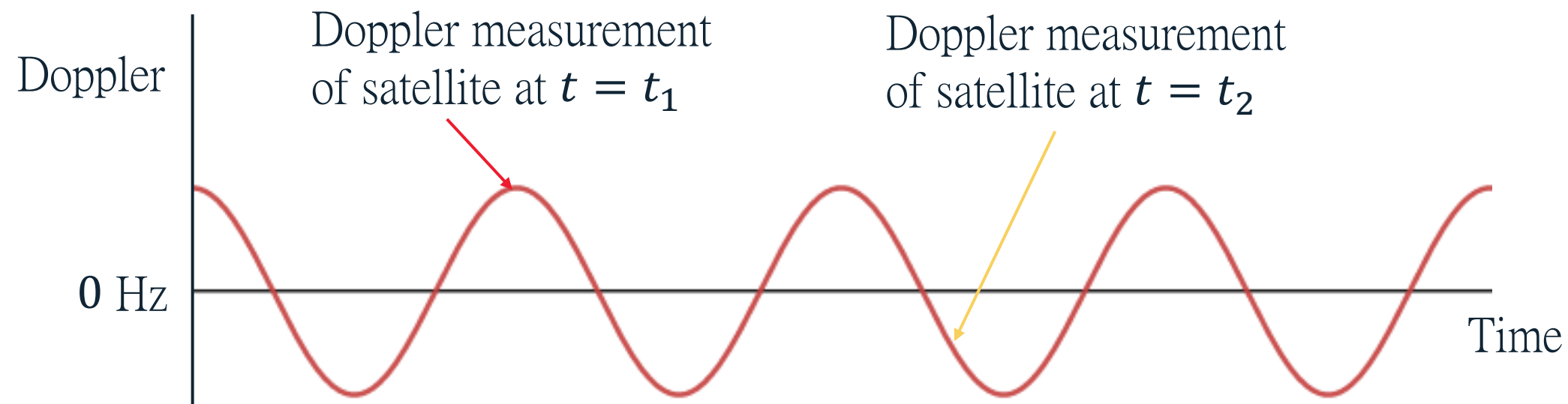


Potential causes for observed perturbations

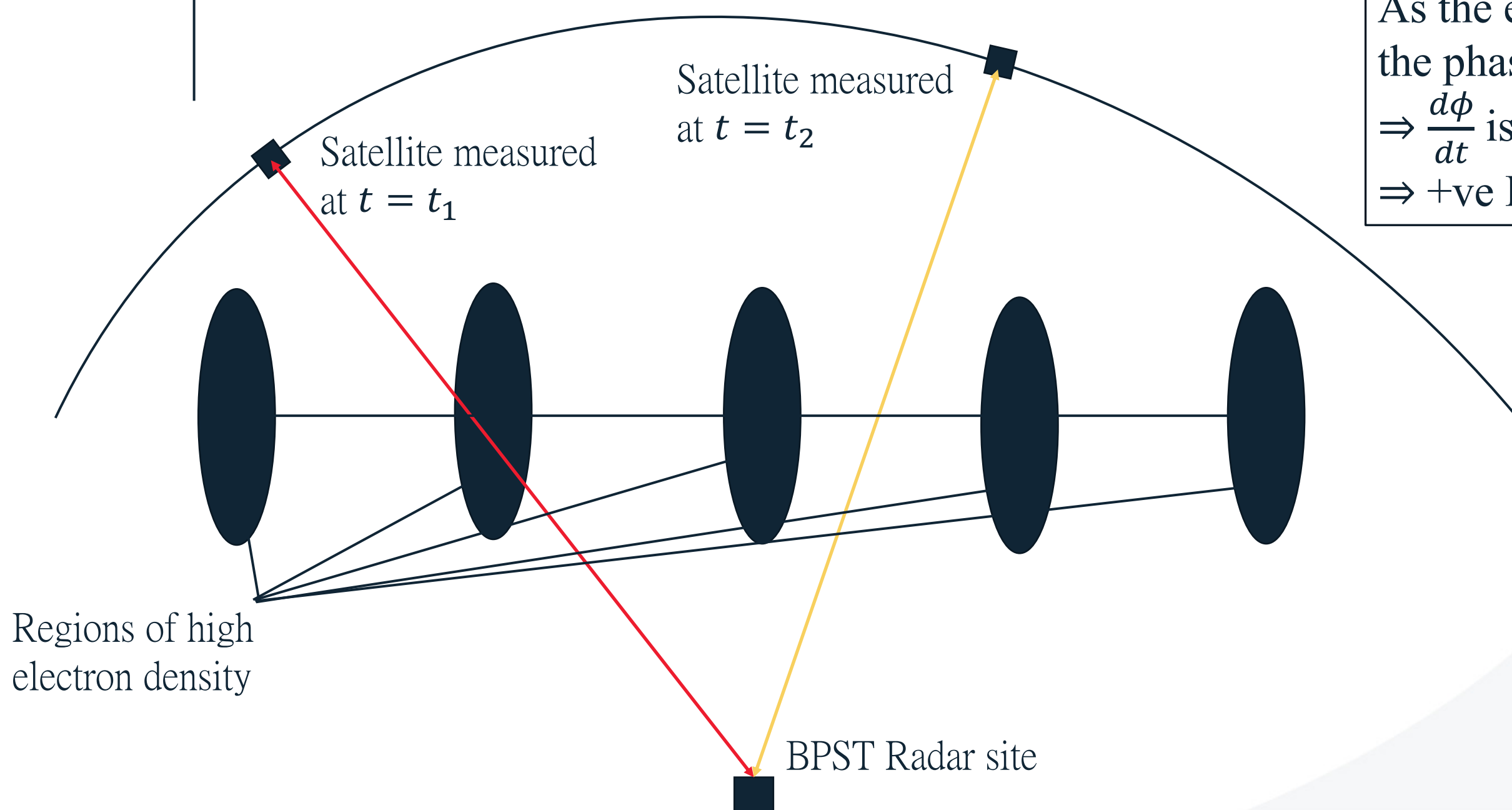
Variation in Doppler due to translational motion has been mostly removed.

Our hypothesis is the Doppler variation is due to an ionospheric effect caused by the radio wave moving through areas of varying electron density.





As the electron density increases
 the phase path decreases
 $\Rightarrow \frac{d\phi}{dt}$ is negative
 \Rightarrow +ve Doppler shift



Potential causes for the ionospheric disturbances

- Atmospheric Gravity Wave (AGW) generated ionospheric disturbances.
 - AGWs are disturbances in the neutral atmosphere, created by many sources.
- Plasma waves generated in the magnetosphere which propagate along geomagnetic field lines to the Earth.



Plasma wave generation regions

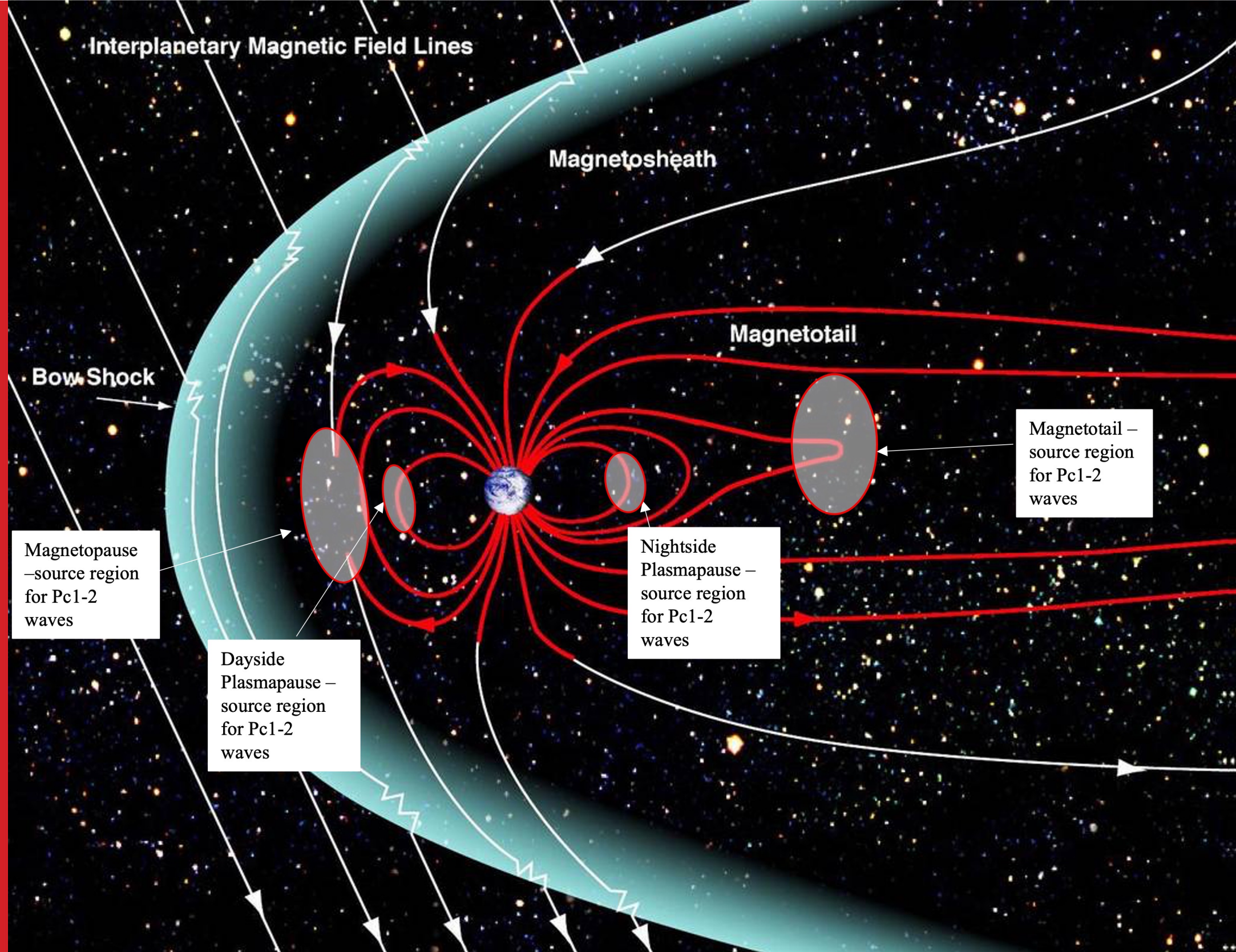
Four generation regions of interest:

Magnetopause – occurrence rate expected to peak at 10:00 and 14:00 MLT.

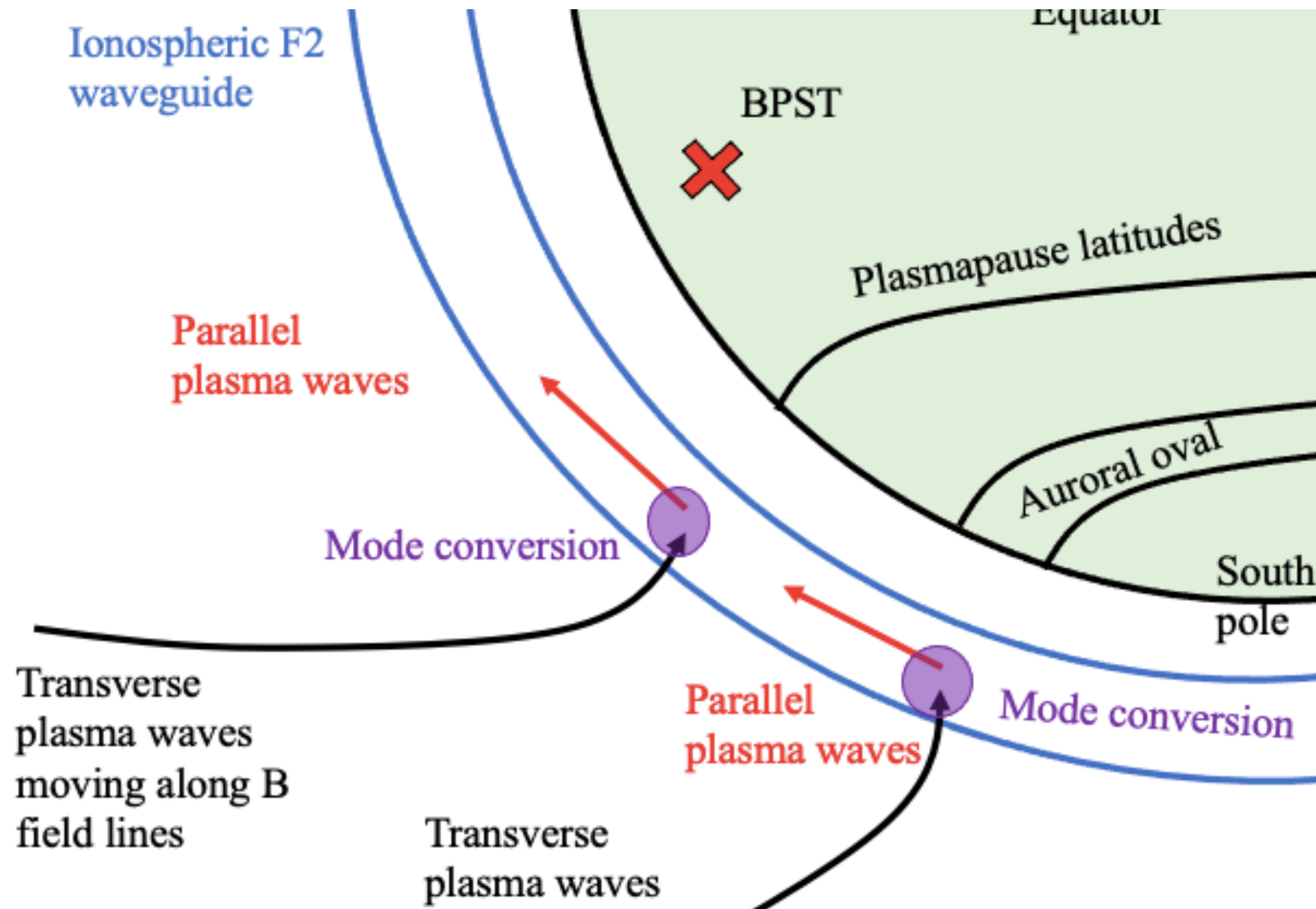
Magnetotail – occurrence rate expected to peak at 00:00 MLT.

Dayside plasmopause – occurrence rate expected to peak at 12:00 MLT.

Nightside plasmopause – occurrence rate expected to peak at 00:00 MLT.



Field line diagram after Zell, 2017

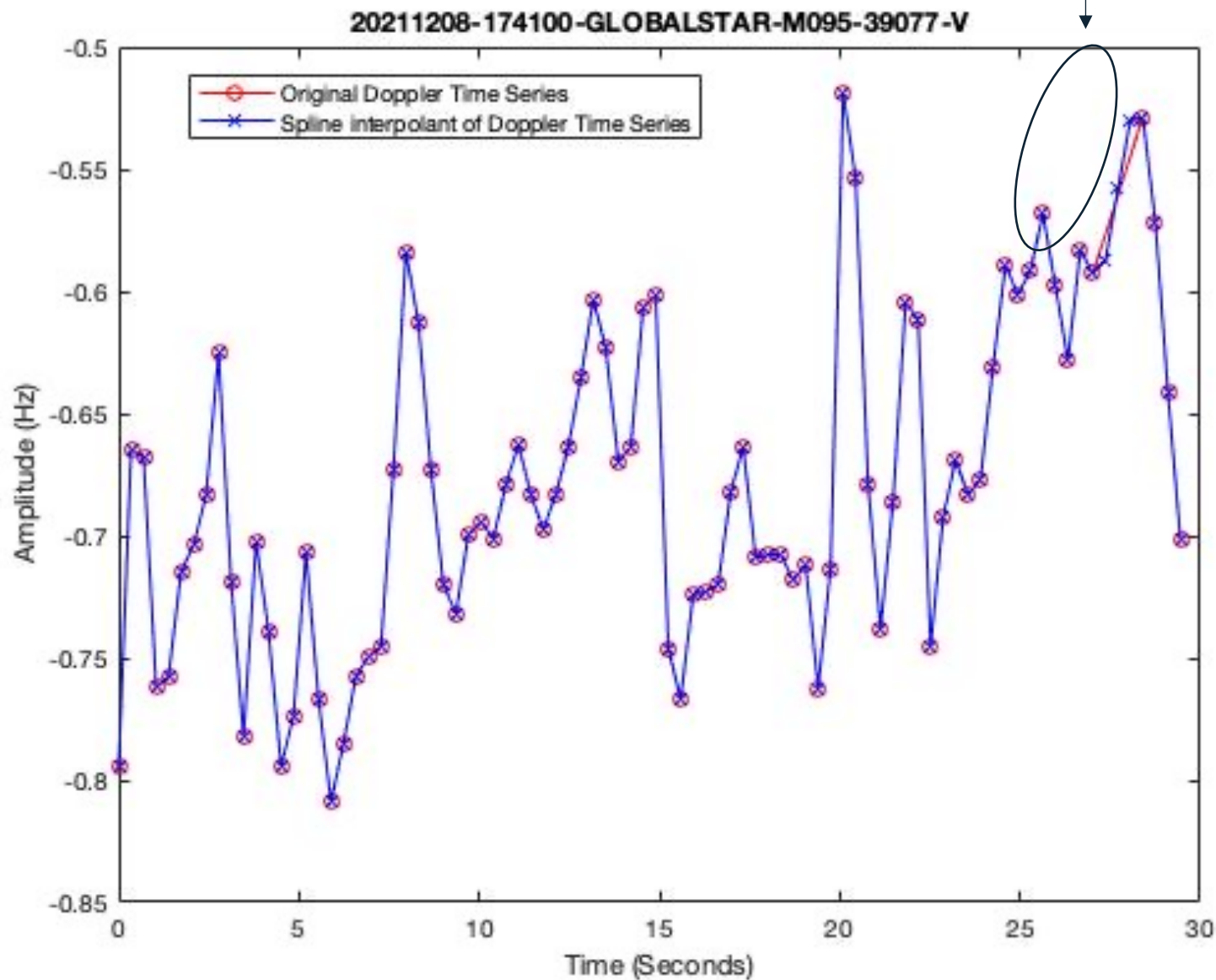


- The plasma waves propagate as transverse waves in the Pc1-2 frequency range until they reach the ionosphere.
- They then mode convert into compressional plasma waves moving in the ionosphere F2 waveguide.

Spectral Peak Detection

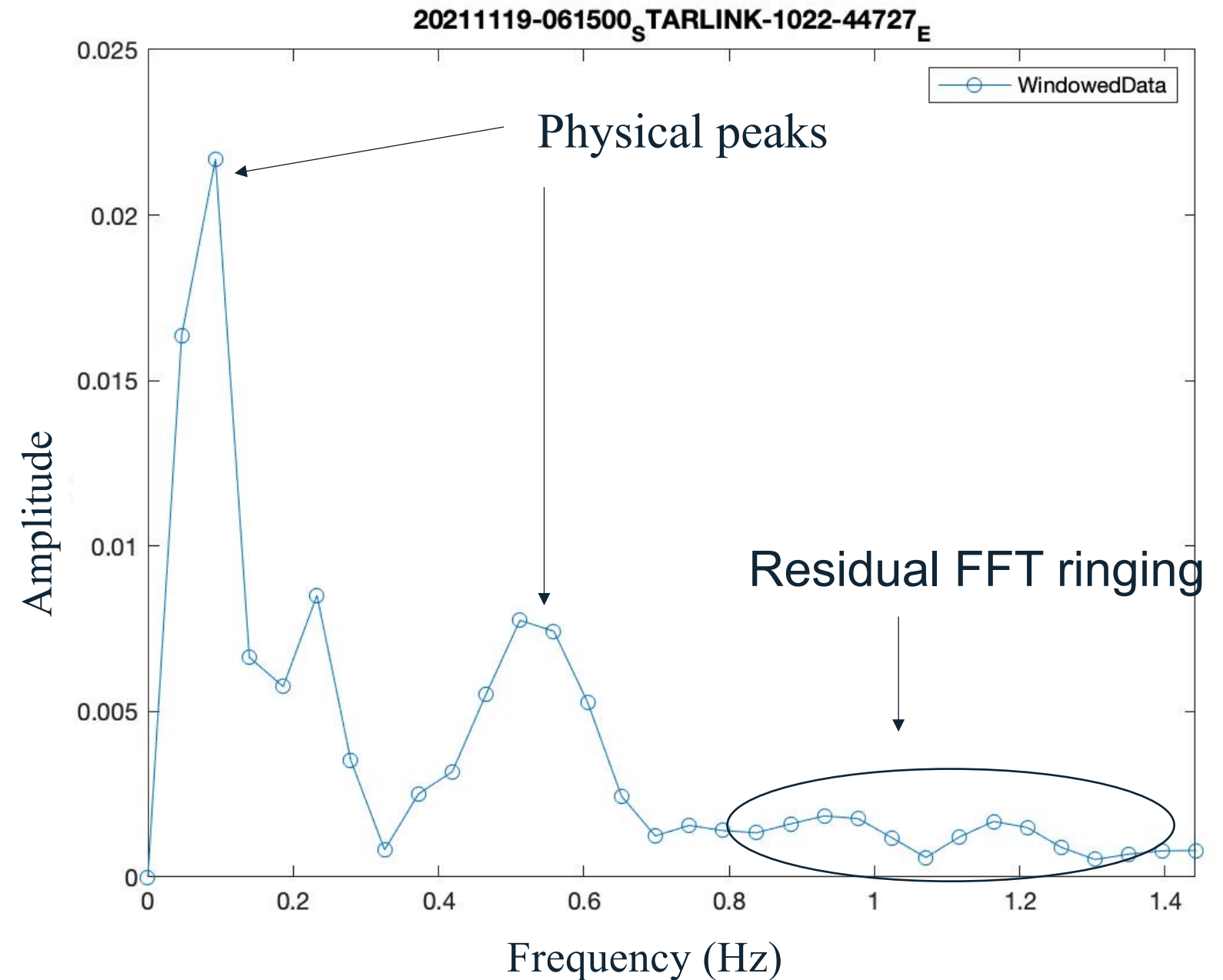
- Cubic spline to resample time series.
- Low pass filter to identify and remove DC component from time series.

Missing data points



Peak detection criteria

Criterion	Value
Minimum Peak Width	0.035
Minimum Peak Height	$H_{min} = (\mu_{1/2}(f(8 : end)) + \bar{x}(f(8 : end)))/2$
Minimum Peak Separation	$f_{sep} = 2.1 * f_{unit}$
Minimum Peak Prominence	0.001



Spectral Peak Detection

The peak detection algorithm:

- Detected 183 peaks.
- Failed to identify 12 peaks.
- Incorrectly identified 4 peaks.

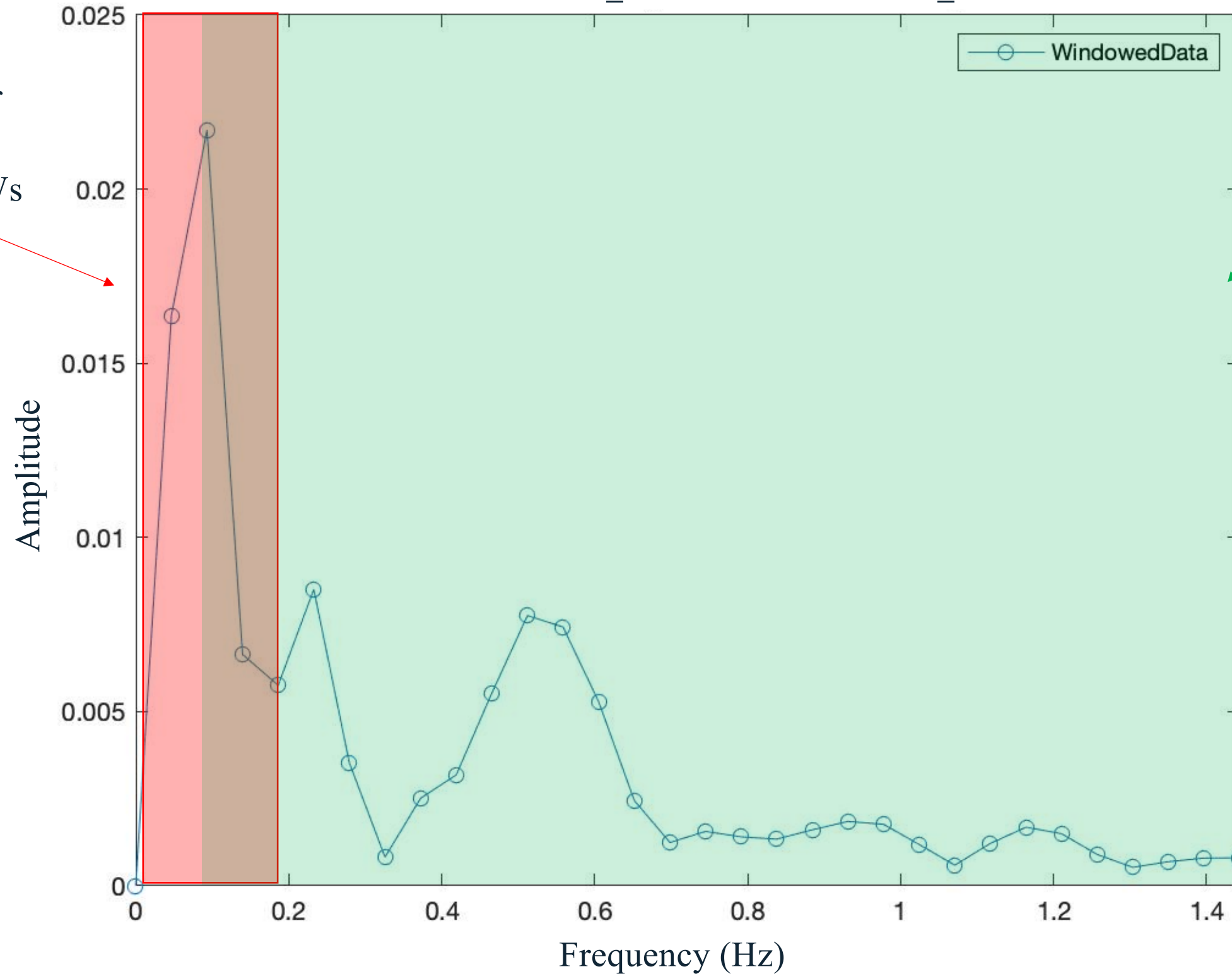
The peak detection algorithm had an accuracy of 91.3%.



Expected Frequencies

20211119-061500_STARLINK-1022-44727_E

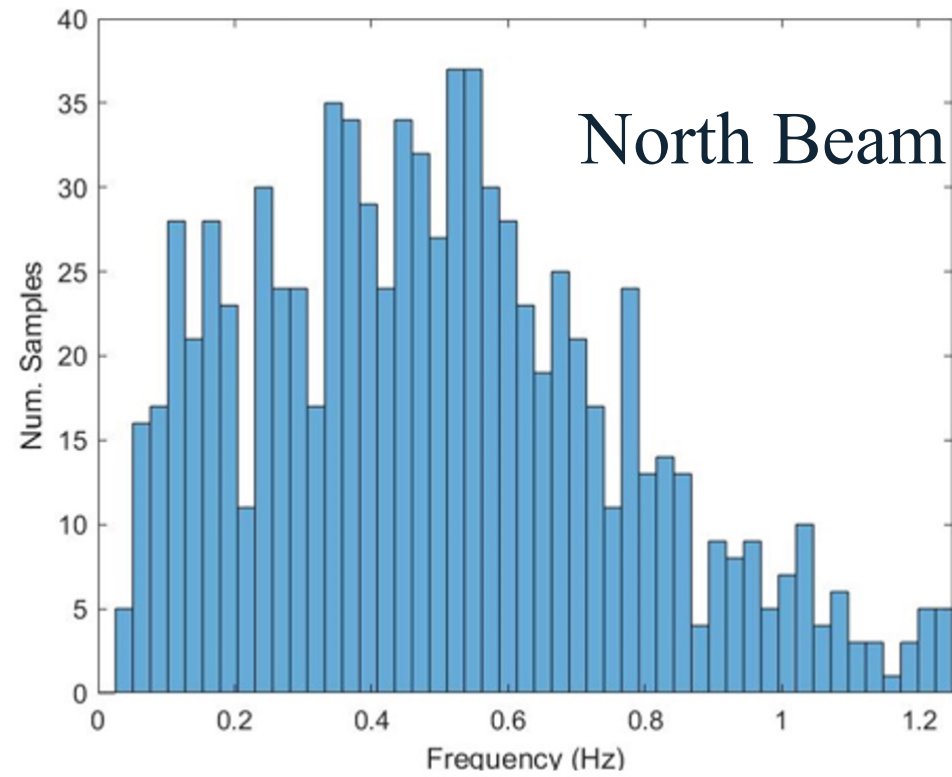
Expected frequency range of medium scale ionospheric disturbances caused by AGWs



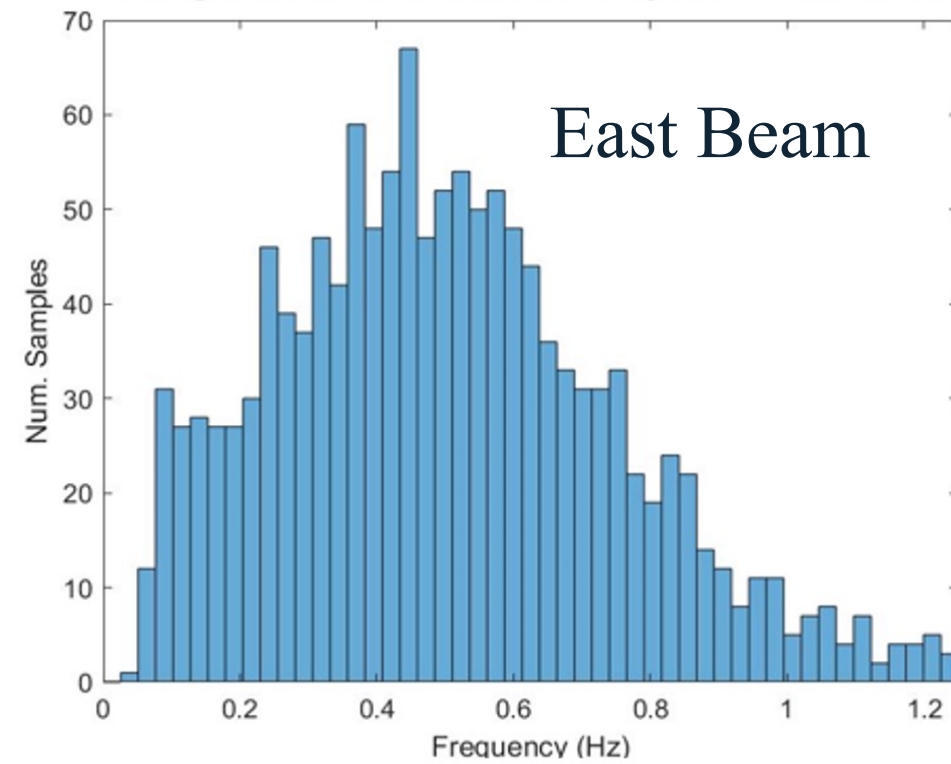
Expected frequency range of the plasma waves

Results - Frequency

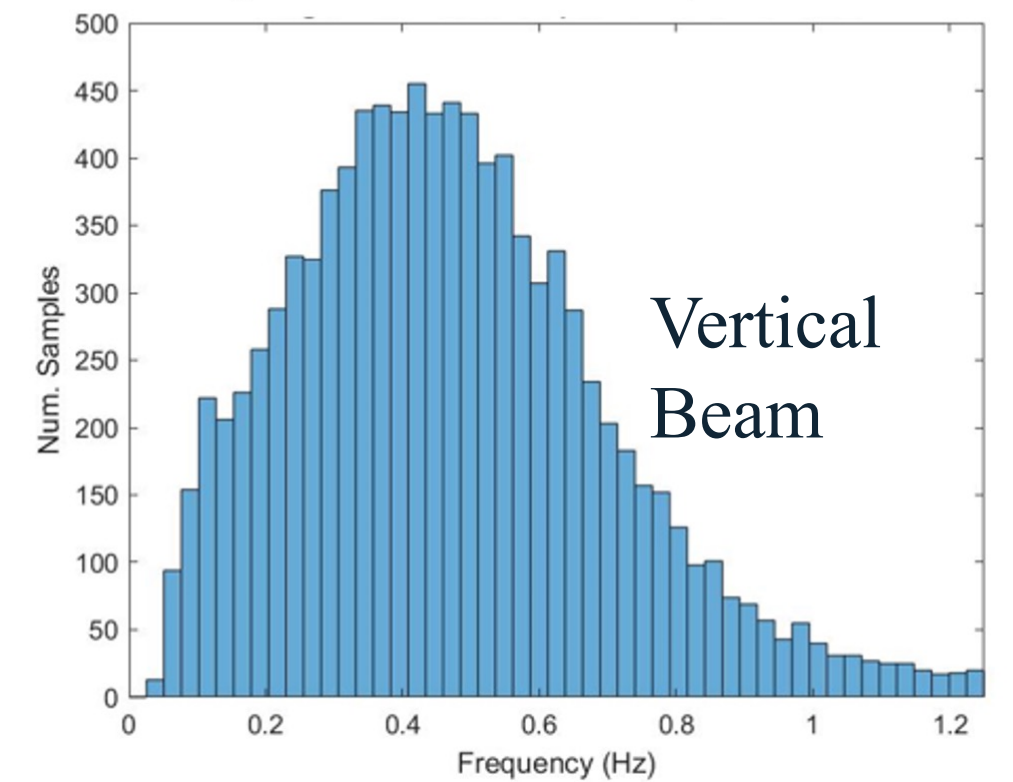
Histogram of observed disturbance frequencies in the N direction



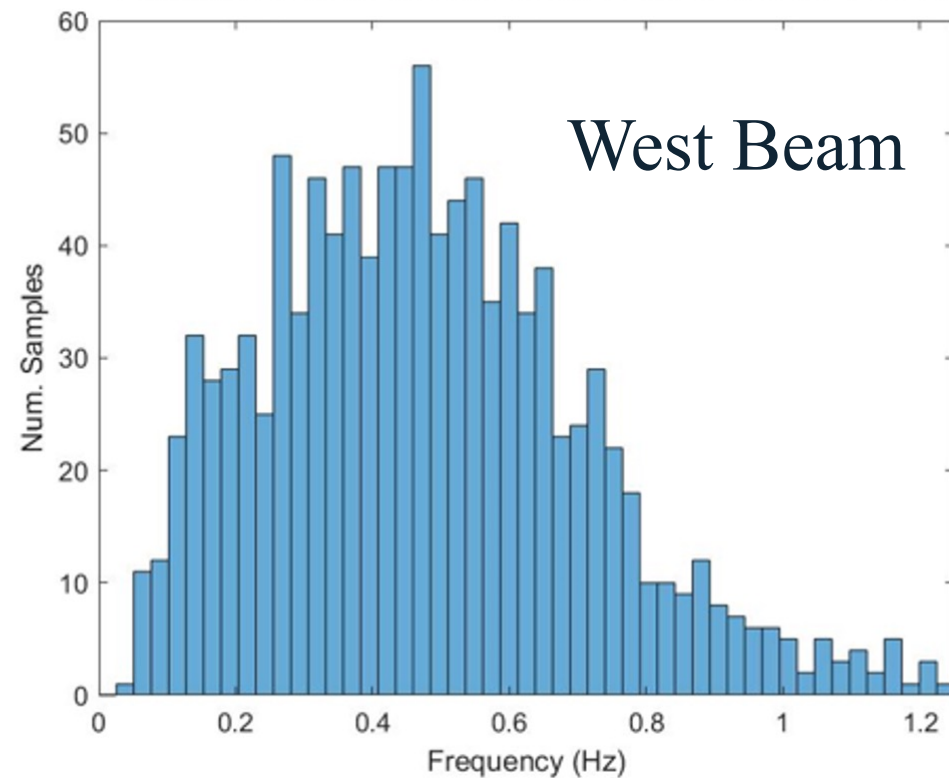
Histogram of observed disturbance frequencies in the E direction



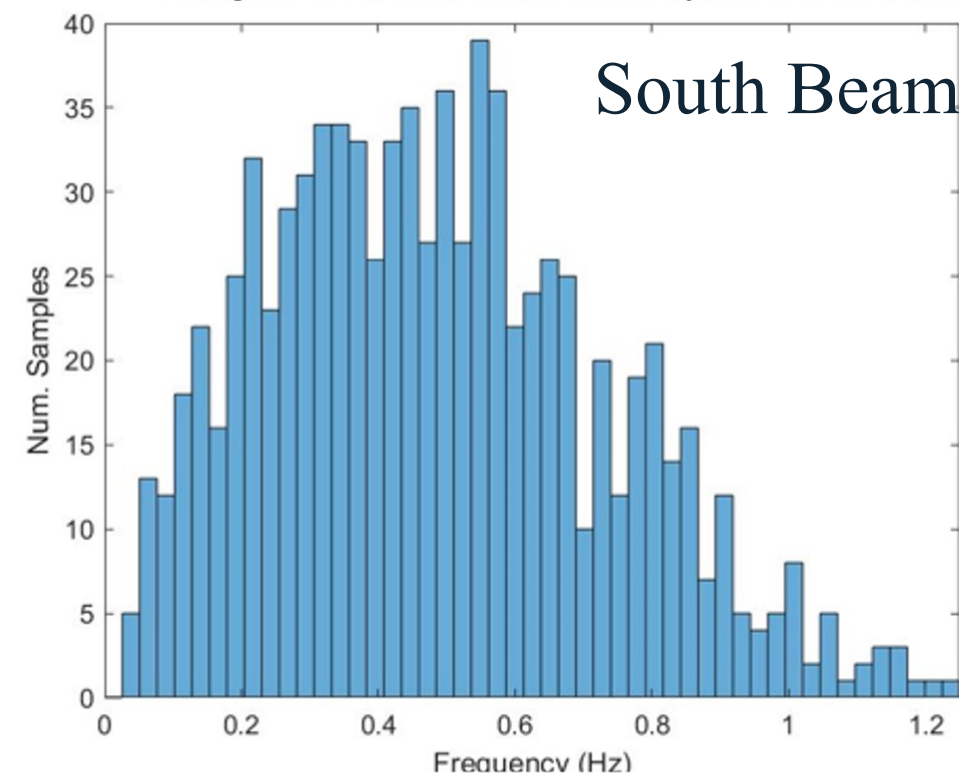
Histogram of observed disturbance frequencies in the V direction



Histogram of observed disturbance frequencies in the W direction



Histogram of observed disturbance frequencies in the S direction

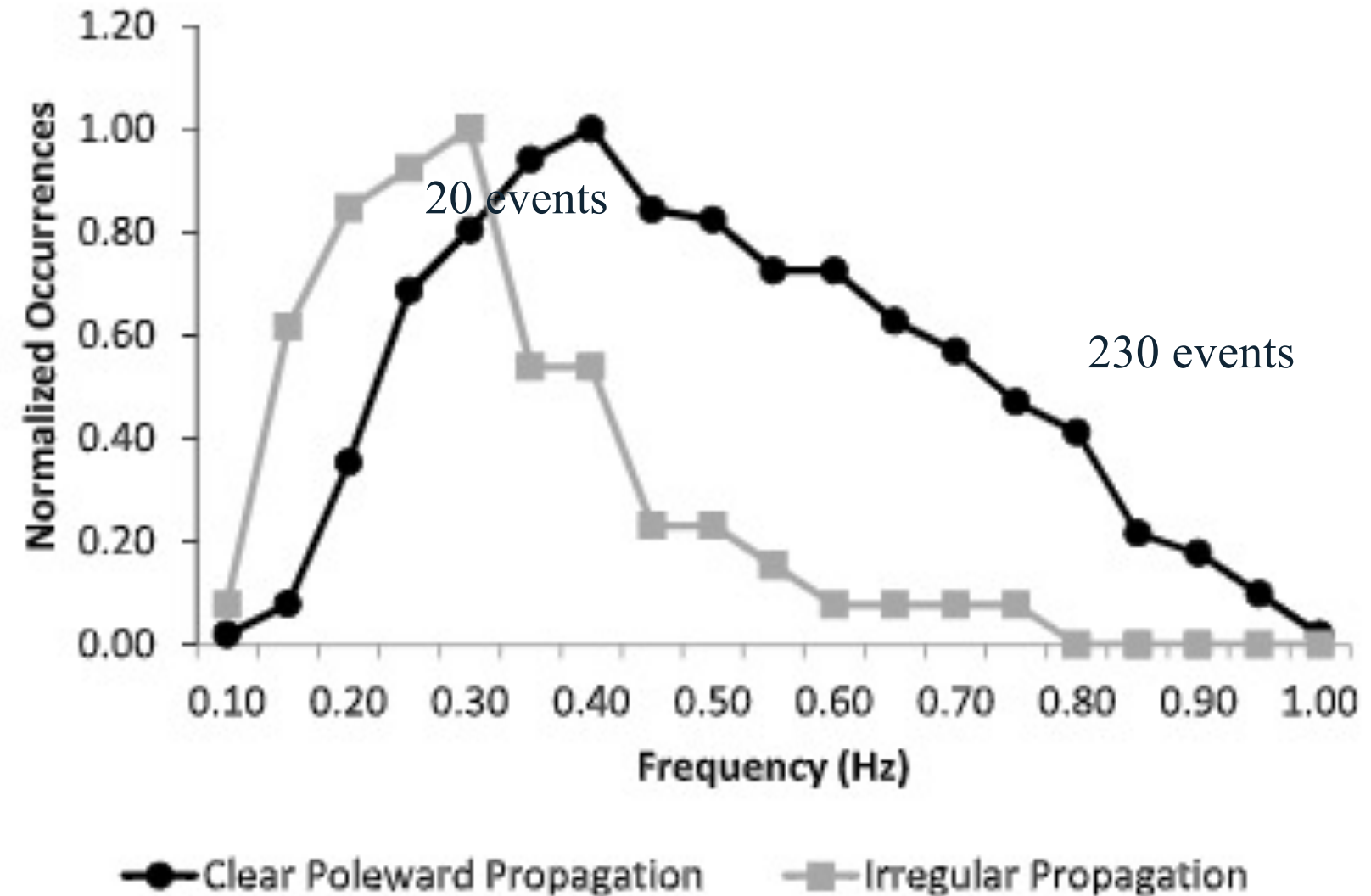
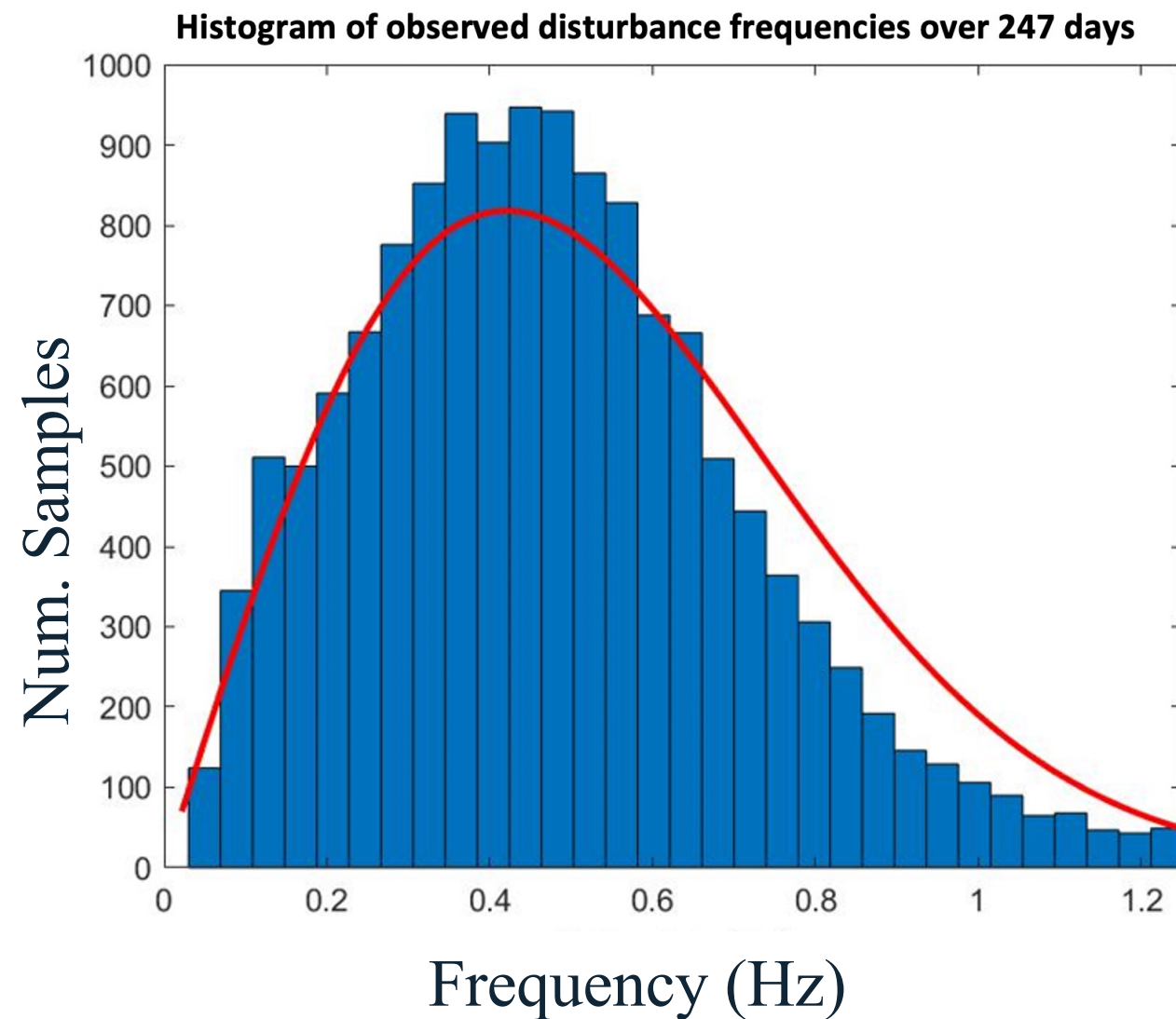


Mode frequency of ~ 0.5 Hz.
Consistent with plasma waves moving in the Pc1-2 range.
Distribution invariant with beam direction.



Results - Frequency

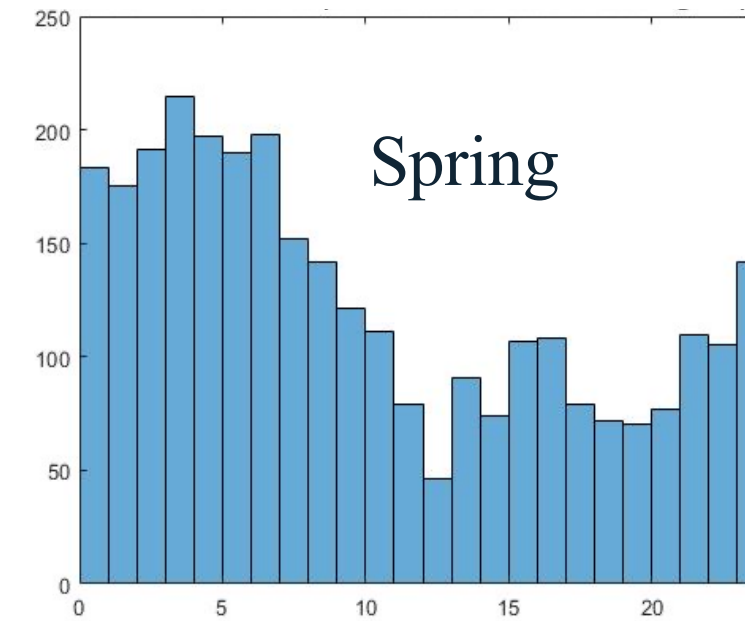
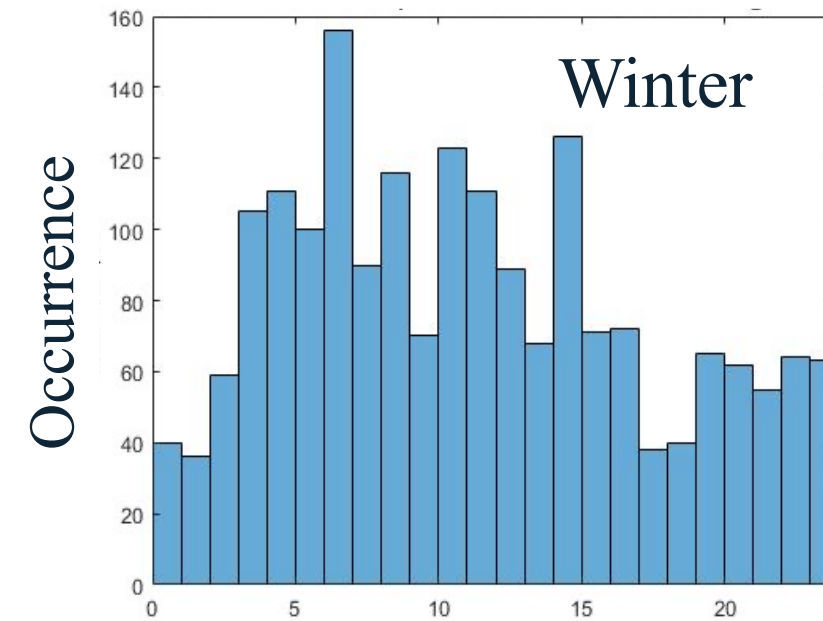
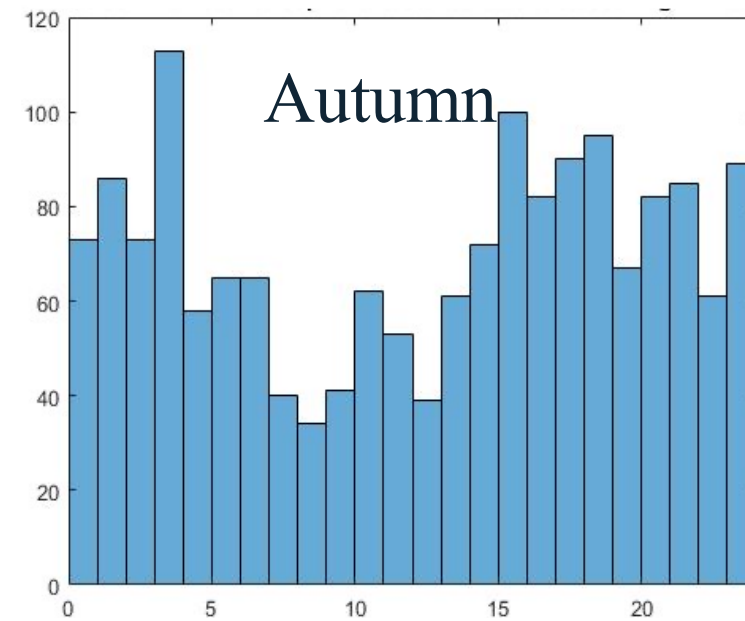
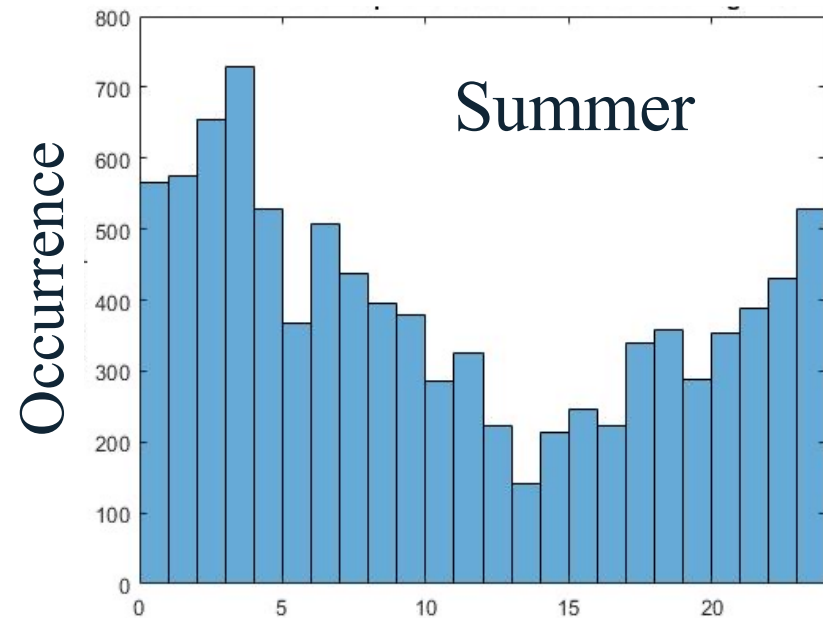
Disturbance frequency is the frequency of the ionospheric disturbance.



After Kim et. Al (2011); ground-based magnetometers measurements inside the Auroral oval

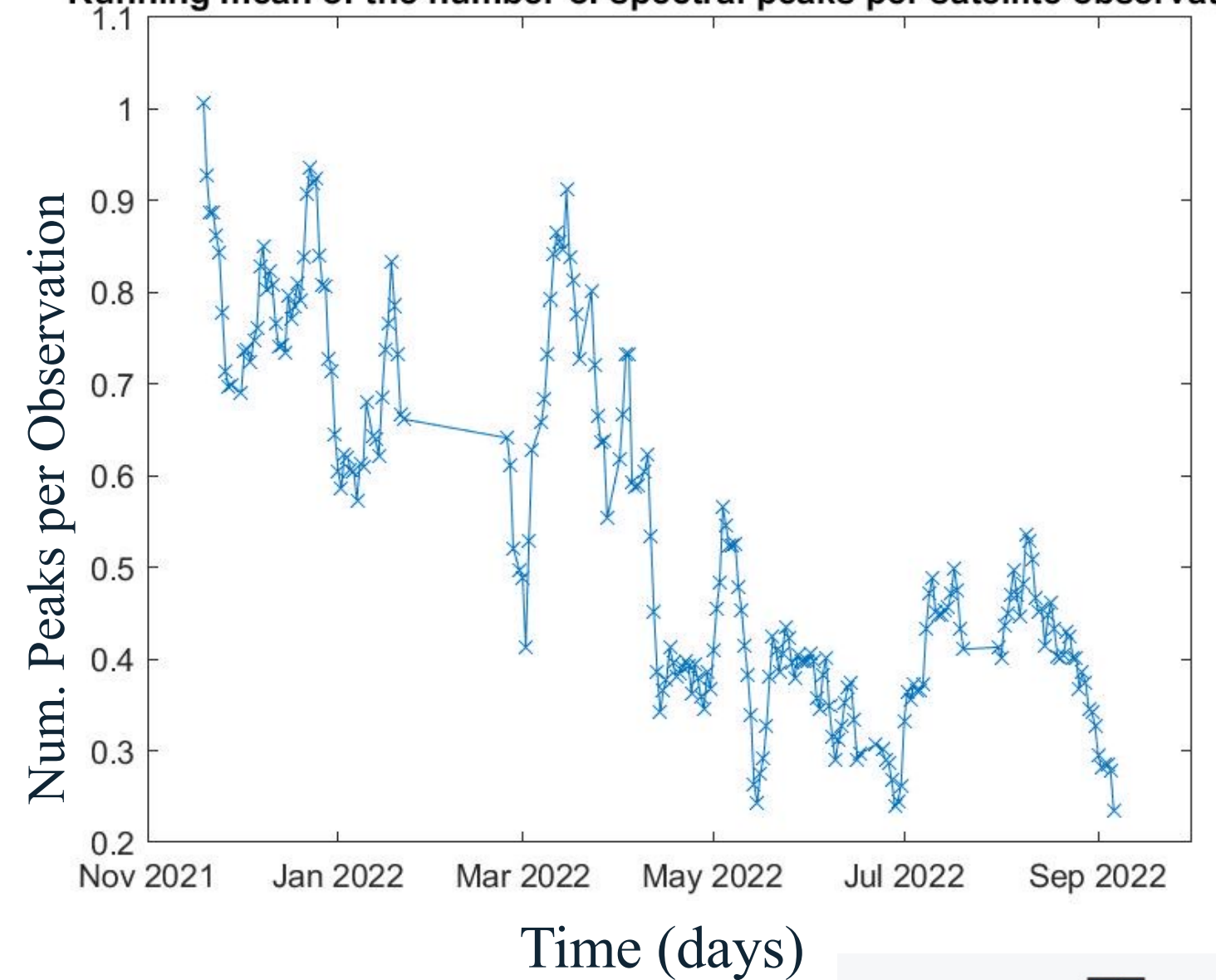
Results – Temporal Variation

Diurnal Variation



Seasonal Variation

Running mean of the number of spectral peaks per satellite observation



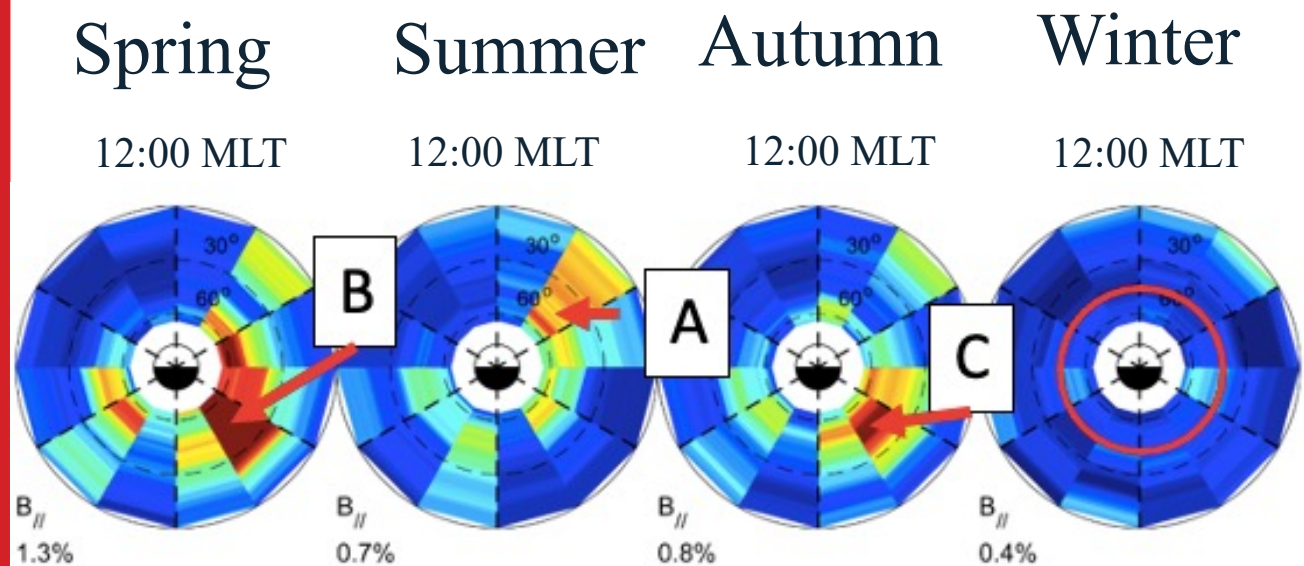
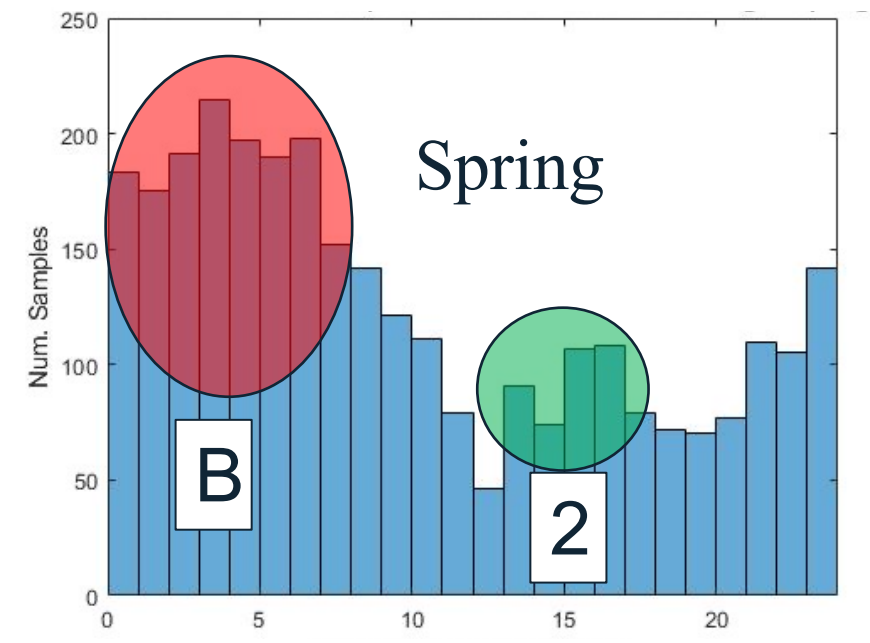
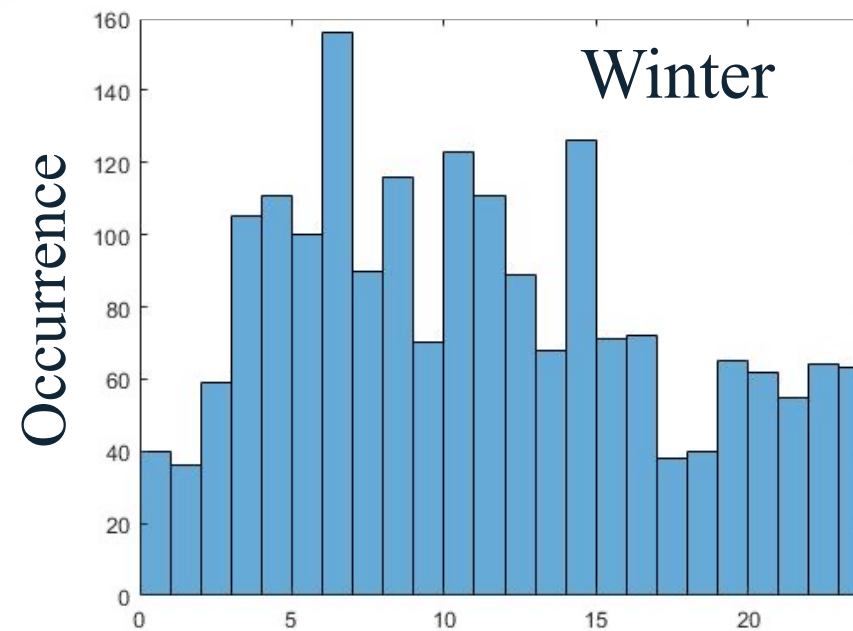
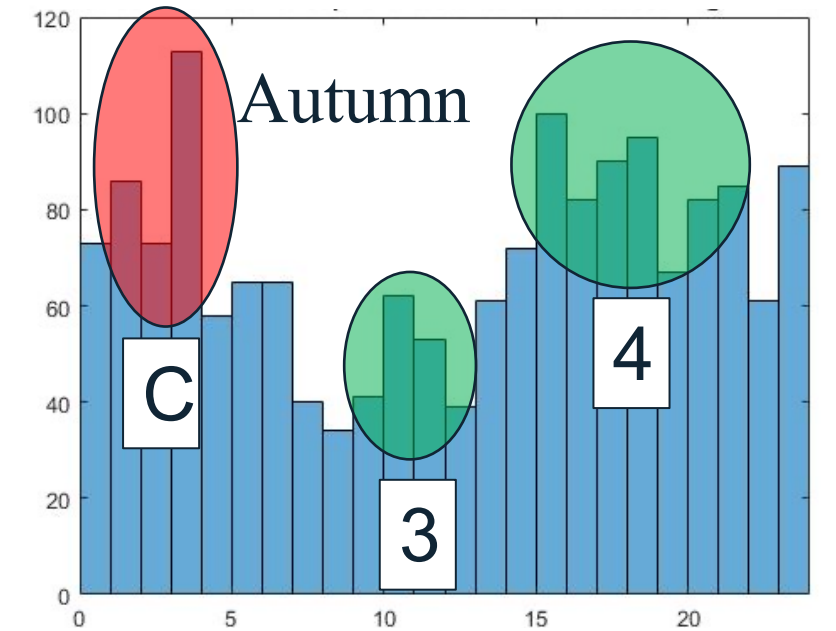
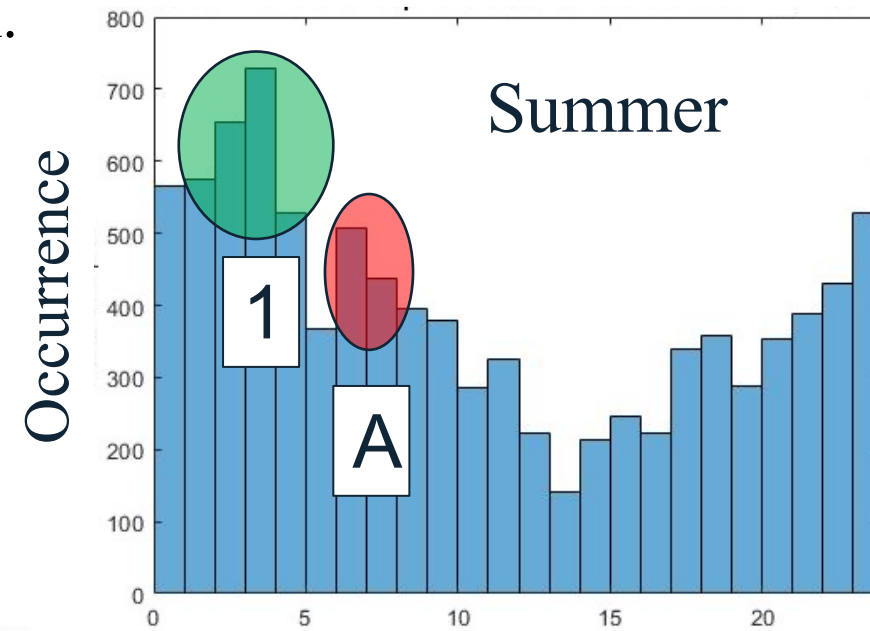
Magnetic Local Time (Hours)

Magnetic Local Time (Hours)

Results – Temporal variation

- Temporal results were compared to Wang et al. 2022 using Swarm satellites.
- BPST observes peaks in the diurnal distributions absent in Wang.
- Wang shows no diurnal distribution during winter
- BPST results show a clear winter diurnal distribution.

- Peaks 1,4, B,C : nightside plasmopause or magnetotail.
- Peaks A and 2 : magnetopause.
- Peak 3 : dayside plasmopause.



Wang et al. (2022); magnetometers onboard satellites

Magnetic Local Time (Hours)

Magnetic Local Time (Hours)

Attenuation in the F2 waveguide

BPST and Wang show preferred source regions for plasma waves; nightside plasmopause, magnetotail and magnetopause.

Due to attenuation in the F2 waveguide.

Attenuation maximized during low electron density as waveguide boundaries reflect plasma waves less efficiently.

Optimal plasma wave generation times may correspond to large waveguide attenuation.

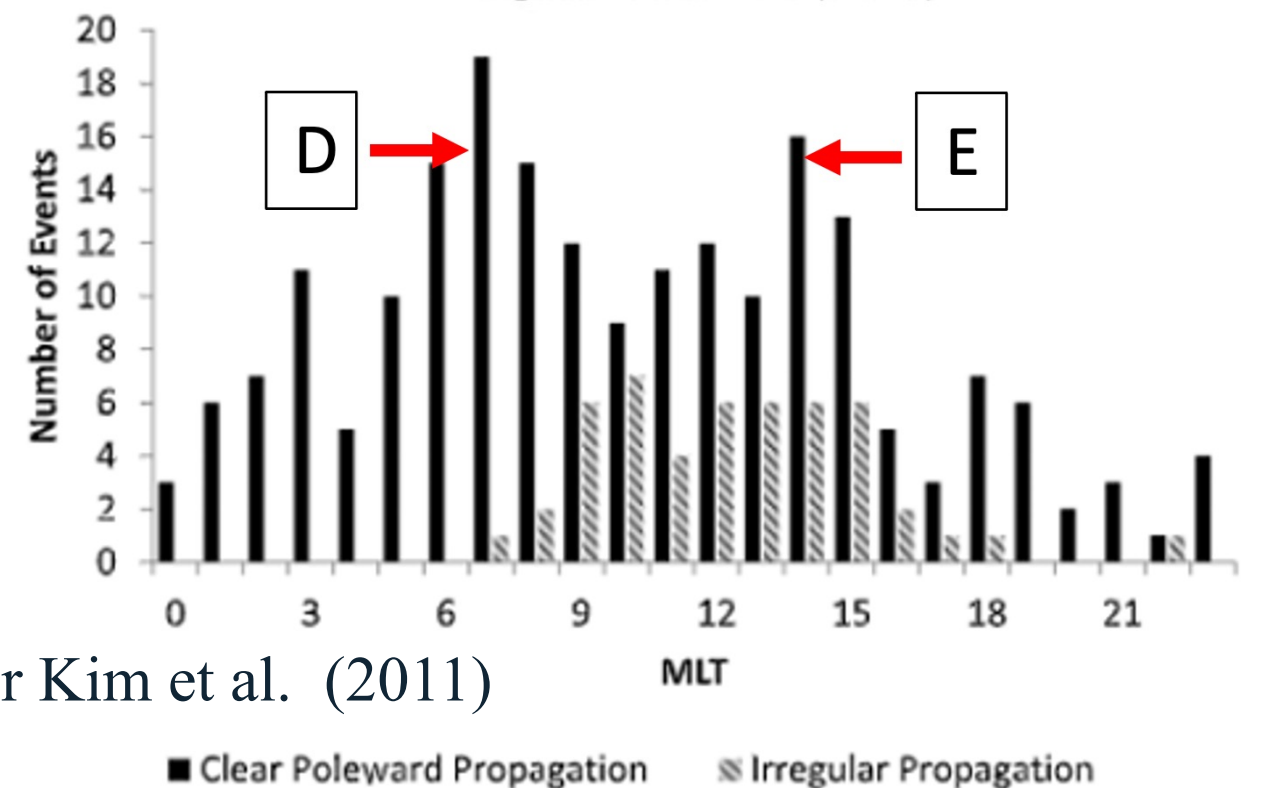
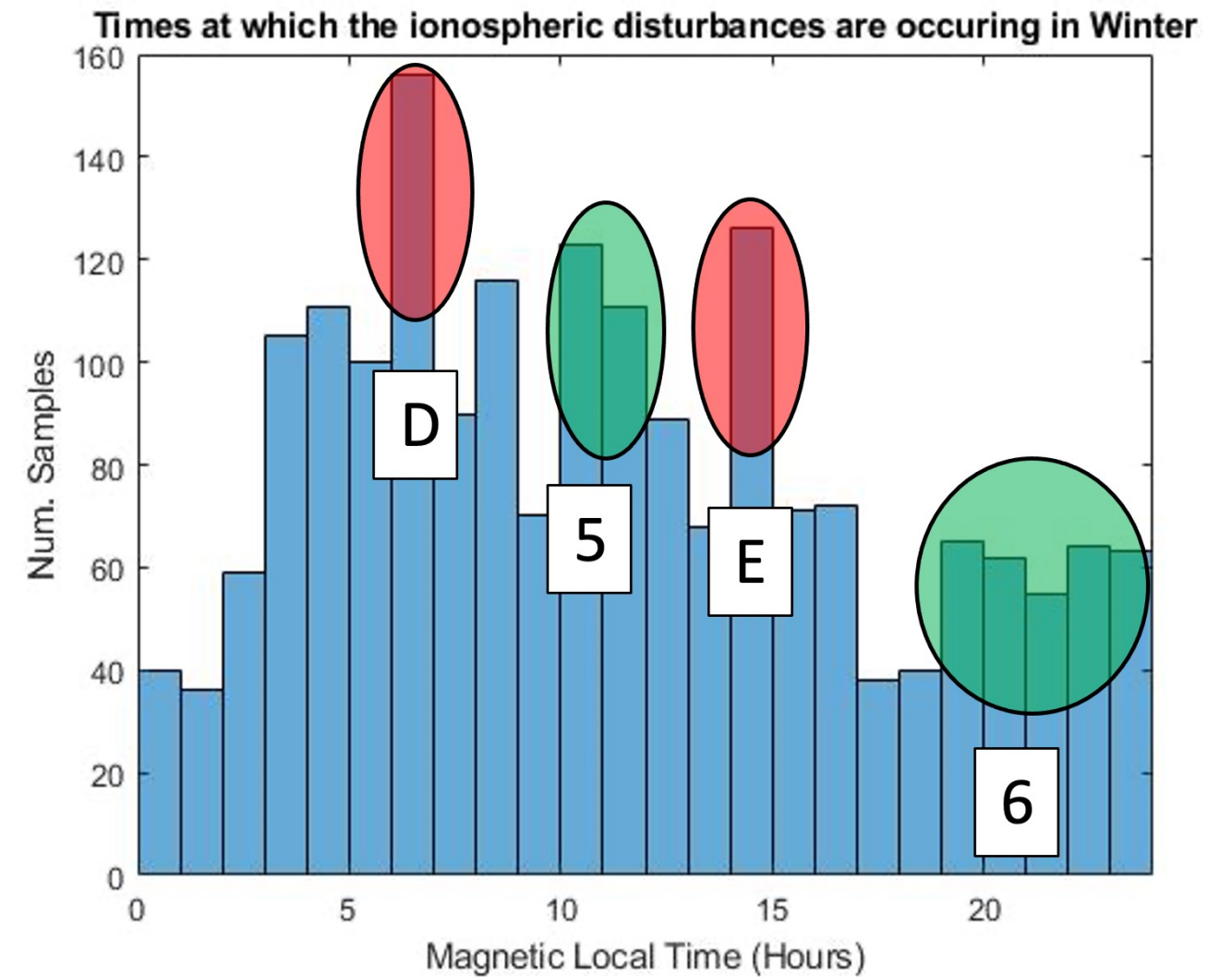
Less optimal times for plasma wave generation may correspond to times conducive to wave propagation.



Results – Winter Diurnal variation

- Winter BPST results compared to Kim et al. using ground-based magnetometers inside the auroral ovals (during all seasons).
- BPST observes peaks that are not present in auroral oval results because the plasmopause generated plasma waves cannot propagate through the auroral oval.

Peaks D, E : The magnetotail.
 Peak 5 : Dayside plasmopause.
 Peak 6 : Nightside plasmopause and the magnetotail.



After Kim et al. (2011)

■ Clear Poleward Propagation ▨ Irregular Propagation

Summary

Fourier analysis was applied to Doppler satellite observations.

A peak finding algorithm was developed and applied to the amplitude spectra.

The spectral results suggest that plasma waves are causing the observed perturbations.

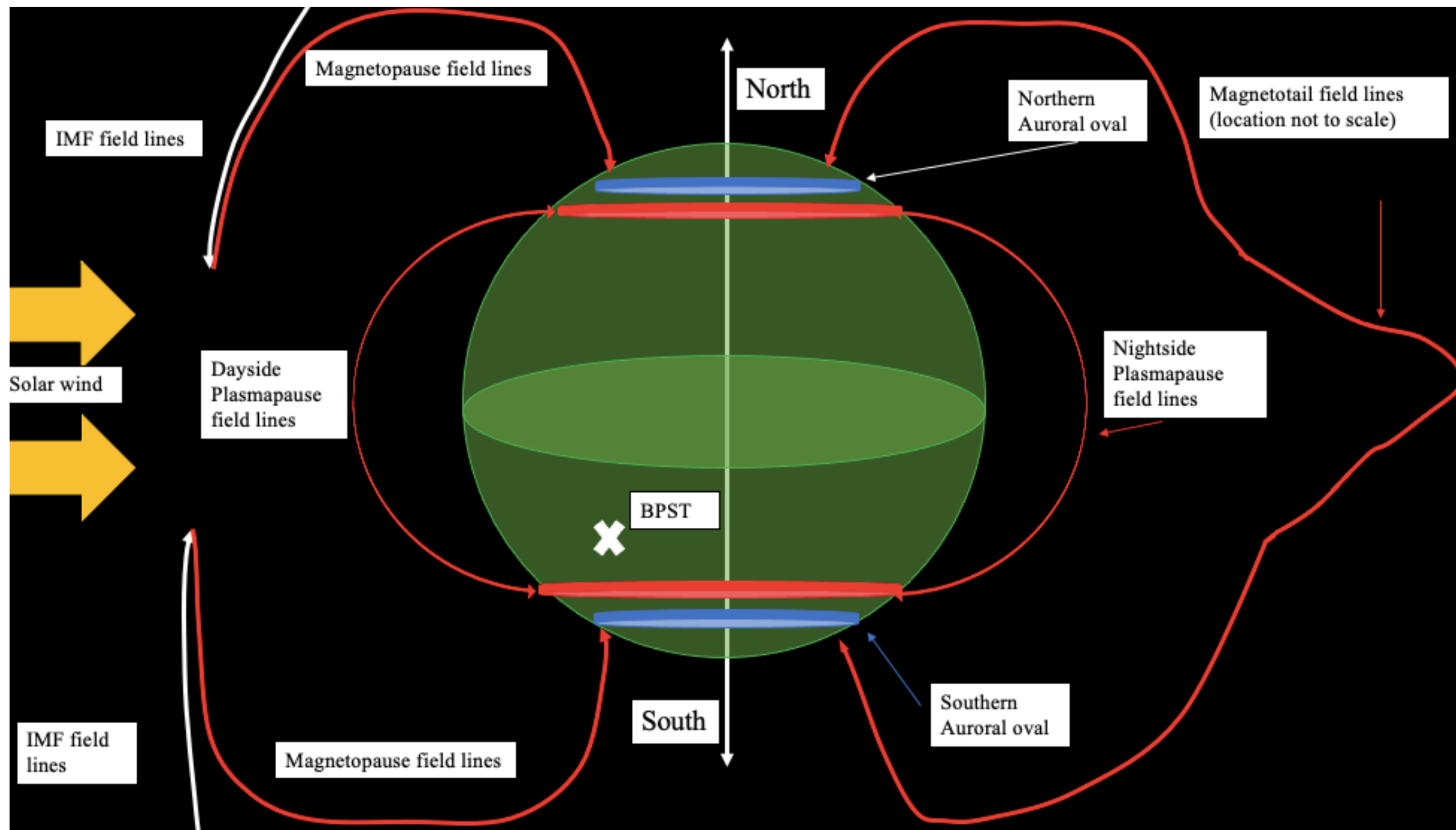
The preferred source regions for these plasma waves are the nightside plasmapause, magnetopause and magnetotail.

The seasonal and diurnal results suggest that VHF radar is more sensitive to the plasma waves than magnetometers.

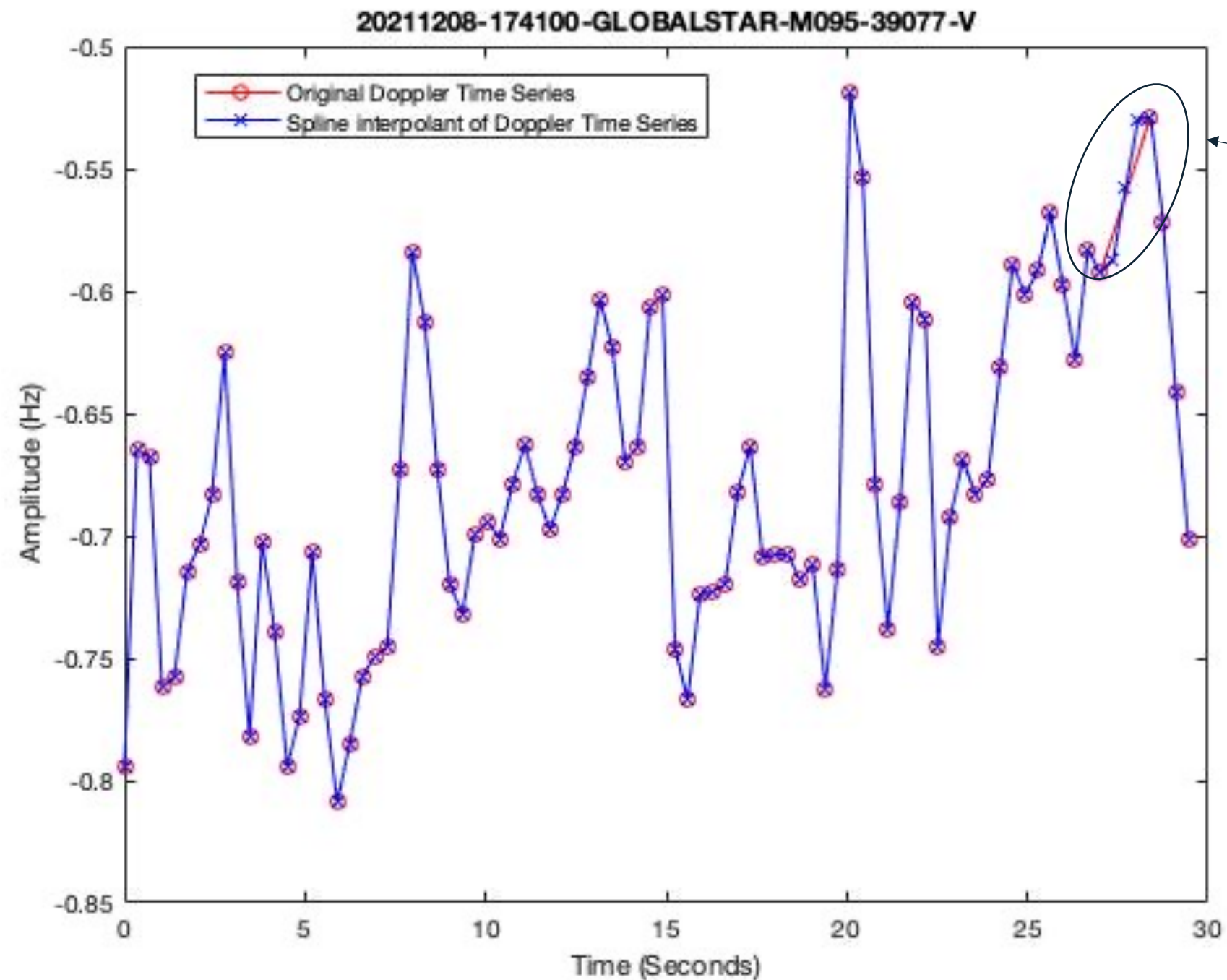




THE UNIVERSITY
of ADELAIDE



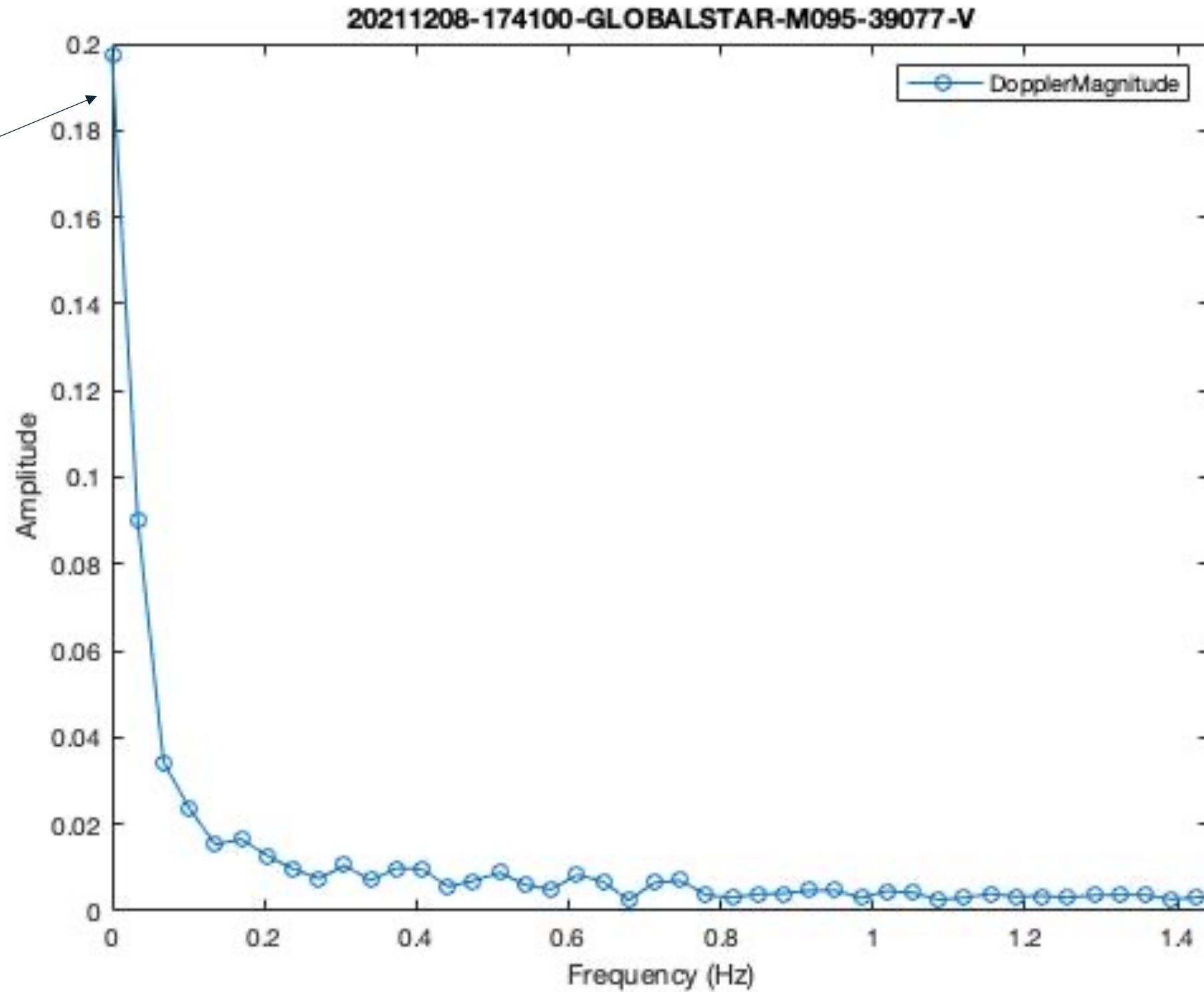
Spectral Analysis of Doppler Peak Data



Missing data p

Spectral Analysis of Doppler Peak Data

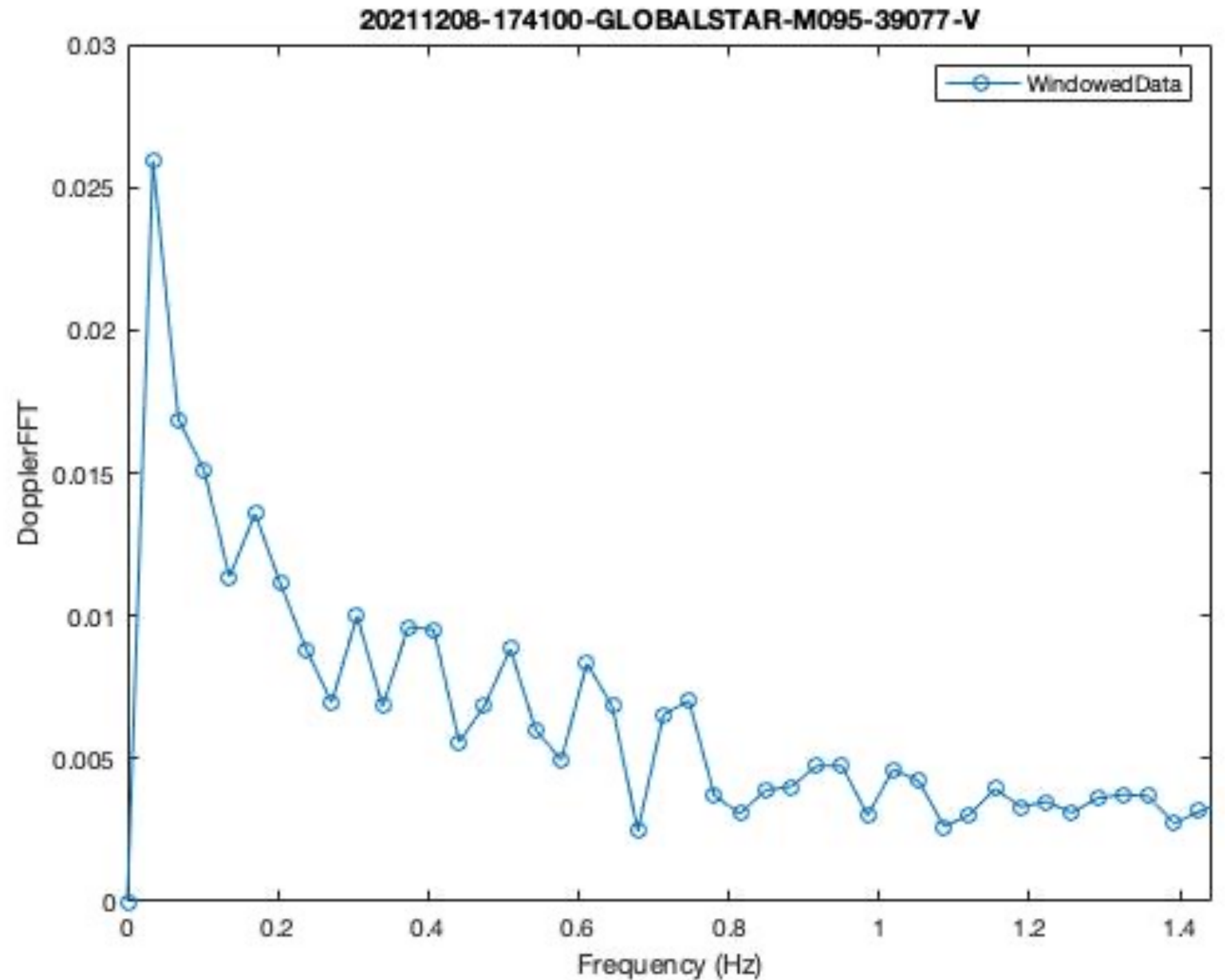
Orbital
Element
Bias



Spectral Analysis of Doppler Peak Data

The low pass filter:

$$y(x) = e^{-10x}$$

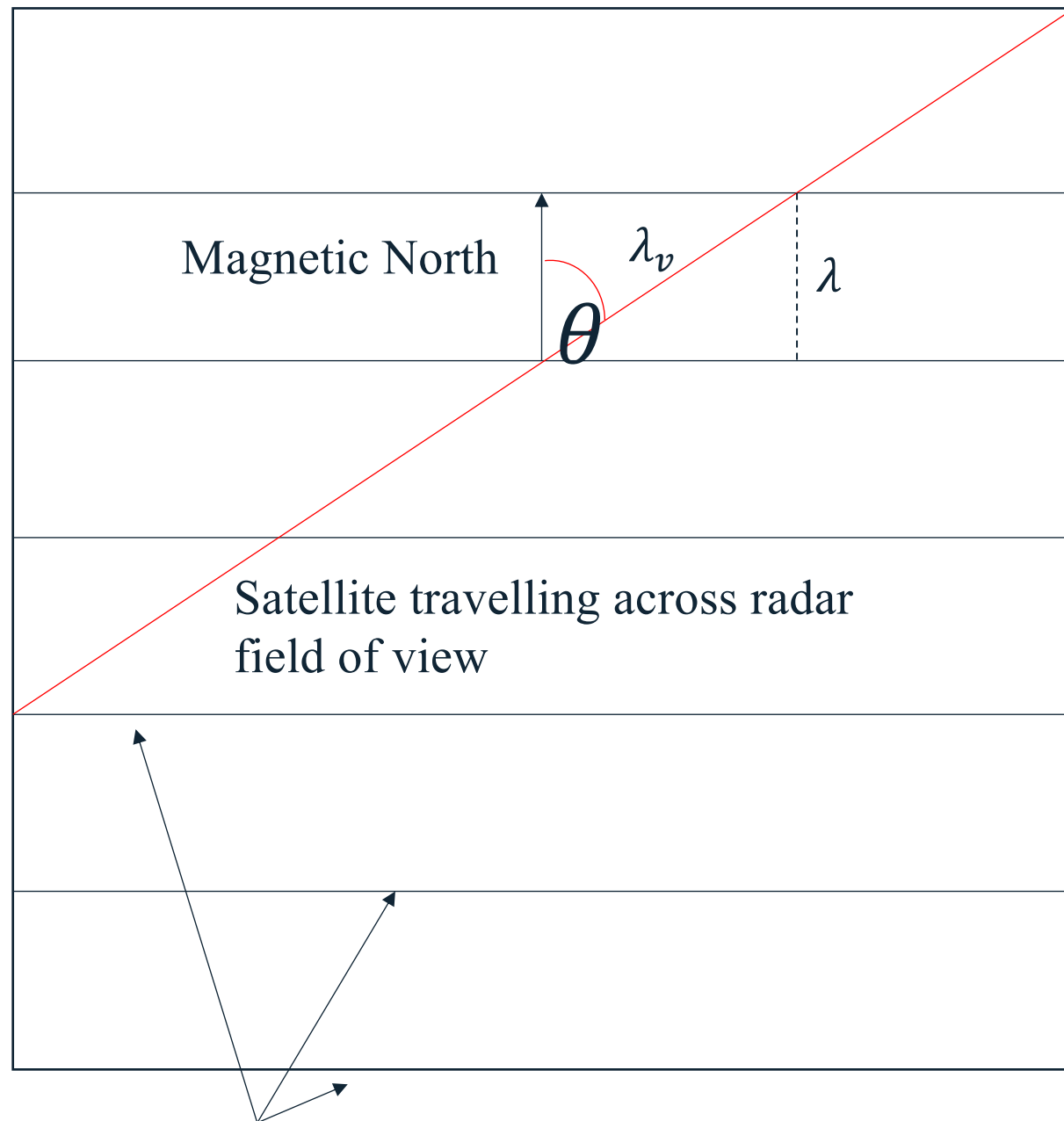


Sensitivity of VHF radar to plasma waves

BPST observing peaks unseen by the Swarm or Antarctic results suggests that VHF radar is more sensitive in detecting the plasma waves than the magnetometers used by the Swarm satellites or Antarctic results.



Frequency Correction



Northward propagating wavefronts

λ_v = virtual wavelength.

λ = true wavelength.

θ = direction of travel with respect to magnetic north.

Conversion from virtual to true frequency:

$$\lambda_v = \frac{1}{\nu_v} \lambda = \frac{1}{\nu} \frac{\lambda}{\lambda_v} = \cos \theta$$

$$\lambda = \lambda_v \cos \theta$$

$$\frac{1}{\nu} = \frac{1}{\nu_v \nu_v} \cos \theta$$

$$\therefore \nu = \frac{\nu_v}{\cos \theta}$$



References

Bennett, J. (Jan. 1967). “The calculation of Doppler Shifts due to a changing ionosphere”. In: Journal of Atmospheric and Terrestrial Physics 29.

Heading, E. et al. (Mar. 2022). “Analysis of RF Signatures for Space Domain Awareness using VHF radar”. In: Institute of Electrical and Electronics Engineers. New York City.

Kim, H., M. Lessard, et al. (July 2011). “Statistical study of Pc1-2 wave propagation characteristics in the high-latitude ionospheric waveguide”. In: Journal of Geophysical Research: Space Physics 116.7.

Wang, H. et al. (Mar. 2022). “Magnetic Local Time and Latitude Distribution of Ionospheric Large-Spatial-Scale EMIC Wave Events: Swarm Observations”. In: JGR Space Physics 127.3.

Zell, H. (Aug. 2017). Earth’s Magnetosphere and Plasmasheet. url: https://www.nasa.gov/mission_pages/sunearth/science/magnetosphere2.html. (accessed: 10.10.2022).

